Supporting Information

Simultaneous identification of viruses and SARS-CoV-2 variants with programmable DNA nanobait

Filip Bošković[1], Jinbo Zhu[1], Ran Tivony[1], Alexander Ohmann [1], Kaikai Chen[1], Mohammed F. Alawami[1], Milan Đorđević [1], Niklas Ermann[1], Joana Pereira Dias[2,3], Michael Fairhead[4], Mark Howarth[4], Stephen Baker[2,3], Ulrich F. Keyser[1,*]

[1] Cavendish Laboratory, University of Cambridge, JJ Thomson Avenue, Cambridge, CB3 0HE, UK

[2] University of Cambridge School of Clinical Medicine, Cambridge Biomedical Campus, Hills Road, Cambridge, CB2 0SP, UK

[3] Department of Medicine, University of Cambridge School of Clinical Medicine, Cambridge Biomedical Campus, Hills Road, Cambridge, CB2 0QQ, UK

[4] Department of Biochemistry, University of Oxford, South Parks Road, Oxford, OX1 3QU, UK

[*] *corresponding author*

This file includes:

Supplementary Text
Figs. S1 to S17
Tables S1 to S29
References

Table of Contents

Section S1. DNA nanobait

Section S1.1 Nanobait design

Nanobait is assembled by mixing linearized DNA scaffold (M13mp18, 7228 nt, Guild Biosciences, 100 nM) with short complementary oligos[3]. A basic set of oligos have 188 oligos 38 nt long and 2 oligos that have 46 nt (with 4 terminal T to avoid aggregation by blunt-end stacking[3–5]) that are complementary to 7228 nt long scaffolds. These oligos are provided in Table S2. Some of the oligos from Table S2 were replaced with oligos that code references (oligos are listed in Table S3) and capture oligos that are specific for five targets. Nanobait has a detection region that is marked by two references and contains five capture strands for five targets (Figure S2a).

Each reference has six interspaced DNA dumbbells (schematic design is shown in Figure S2b) i.e. DNA double hairpins (5'-TCCTCTTTTGAGGAACAAGTTTTCTTGT-3') that is interpreted as one downward signal in nanopore events[6,7]. In addition to capturing oligo (38 nt complementary to DNA scaffold and 20 nt complementary to target), each capture site contains partially complementary oligo (14 nt) that carries a label (Figure S2c). This free single-stranded part of the capture strand contains a toehold (6 nt) for strand displacement reaction. Once a target is added to the solution, the target first binds to the toehold and then displaces the oligo with a label (Figure S2d). Hence, target presence is detected as the absence of oligo with a label (missing peak in a nanopore event).

Section S1.2 Linearization of circular single-stranded M13

Linearization of circular M13 scaffold (M13mp18, 7249 nt) is performed using double restriction digestion. Firstly, we bound an oligonucleotide (39 nt long, 5'-TCTAGAGGATCCCCGGGTACCGAGCTCGAATTCGTAATC-3') to the scaffold to create a double-stranded region for efficient enzyme digestion. Such a double-stranded region contains closely spaced restriction sites for EcoRI and BamHI enzymes. The double enzyme digestion is used to ensure complete linearization of the scaffold. We mixed 52 µL of scaffold (M13mp18, 100 nM) with 10 µL of 10 × CutSmart buffer (1 × buffer components are 50 mM potassium acetate, 20 mM Tris-acetate, 10 mM magnesium acetate, 100 µg/ml BSA, pH 7.9 at 25 °C; New England Biolabs), 2.5 µL of 39 nt long oligo (100 µM in H_20, IDT), and 33.5 µL of filtered Milli-Q water. The mix was heated to 65 °C for 30 s and slowly cooled down to 25 °C over ~40 min. After oligo binding, 1 µL of EcoRI-HF enzyme (100.000 units/mL) and1 µL of BamHI-HF enzyme (100.000

units/mL) was added to the reaction and mixed by pipetting the full volume multiple times and incubated at 37 °C for 1 h. The cut scaffold was purified as previously described using NucleoSpin Gel and PCR Clean-up kit (Macherey-Nagel™)[3].

Section S1.3 Nanobait assembly

Nanobait is assembled by mixing the scaffold with a respective set of oligos. Briefly, we mixed 800 fmoles of the linearized scaffold with three times excess of oligos (2400 fmoles each) in 10 mM $MgCl_2$, 1 × Tris-HCl, pH 8.0. The reaction was heated to 70 °C for 30 s followed by linear cooling to 25 °C over 45 min. The excess oligos were removed with Amicon 0.5 mL filters with 100 kDa cut-off using washing buffer (10 mM Tris-HCl, pH 8.0, 0.5 mM $MgCl_2$). The samples were centrifuged at 9,200 × g for 10 min twice, and after the filter was inverted, placed in a new tube, and spun down at 1,000 × g for 2 min. Nanobait concentration was estimated from a NanoDrop spectrophotometer or a Qubit fluorometer using Qubit™ dsDNA BR Assay Kit.

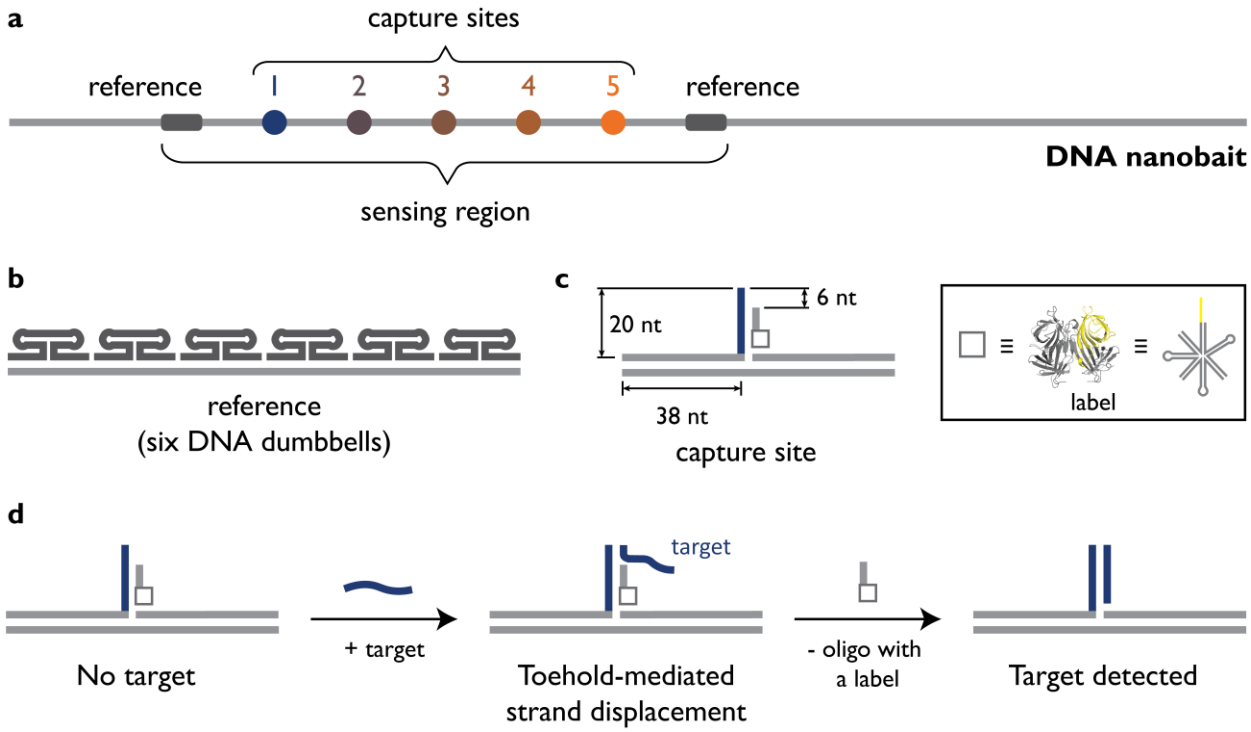

Figure S1. DNA nanobait schematic design. a) Nanobait contains a detection region that has two references (dark gray) and five capture sites for each target strand. b) Reference represents six DNA dumbbells that are interspaced and are read as one downward signal in nanopore

measurements. c) Capture site structure is represented by capture strand that has 38 nt part complementary to DNA scaffold and 20 nt part that is fully complementary to a target strand. Oligo that carries label is partially complementary to capture strand (14 nt). Label can be either monovalent streptavidin or DNA flower. d) The uncomplemented part of the capture strand (6 nt) is called the toehold and it serves as a seed for displacement (removal) of the oligo with a label if the target is present.

Section S2. Design of structural labels used for nanopore signal amplification

Specific identification of the presence or absence of the target sequence in solution is done by using nanopore sensing. In nanopore recordings, the "control" or absence of a target is detected as a downward signal or peak on a DNA event. This peak corresponds to a label that is attached to an oligonucleotide (oligo or strand) (further explained in Section S3). In this study, we demonstrated that both protein-based and DNA-based structures can be employed as labels.

As a protein-based label, we employed monovalent streptavidin (structure shown in Figure S1a) that has a single femtomolar biotin binding site. Monovalent streptavidin expression and purification have been described previously[1]. Oligos have a biotin label on the 3' end via a C6 spacer arm (Integrated DNA Technologies) to which monovalent streptavidin binds.

As a DNA-based label, we assembled a DNA flower[2] that represents a 7-way junction as is illustrated in Figure S1b using four DNA strands as described in the next section. One of the strands (J4, Table S1) has 14 nt single-stranded part (in grey) that is used as an anchor that binds to nanobait (explained in Section S3).

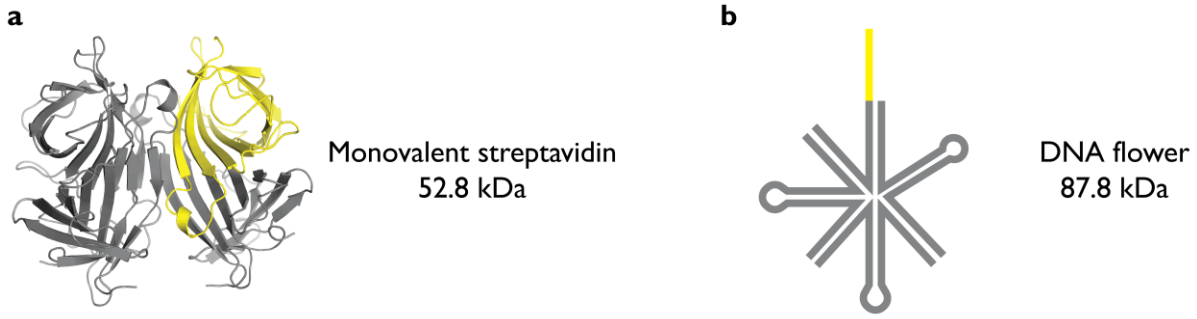

Figure S2. The designs of structures used in this study as labels. a) The tetramer is formed from one biotin-binding subunit in yellow and 3 non-binding subunits in gray (PDB ID: 5TO2). b) DNA flower represents a 7-way junction, design with an arm length of 16 bp and loops with 4 T (gray). Oligo that binds to a respective site on the nanobait is in yellow.

Section S3. DNA flower synthesis

Three DNA flowers specific for each SARS-CoV-2 target (7-way junctions, 7WJa, 7WJb, and 7WJc) were prepared separately. Taking 7WJc as an example, 4 μM DNA strands J1, J2, J3, and J4c (Table S1) were mixed in TM buffer (10 mM Tris-HCl, 10 mM $MgCl_2$, pH 8.0) and heated at 90 °C for 5 min, then cooled down to 65 °C for 15 min, 45 °C for 15 min, 37 °C for 20 min, 25 °C for 20 min and finally 4 °C for 20 min. Strand J4c was substituted by J4b to prepare 7WJb. For 7WJa, to avoid self-folding and improve the occupied fraction at site 43 on nanobait, J1, J2, J3 J4a, and C43 were mixed before annealing.

Supplementary Table S1. DNA flower oligonucleotides. The complementary parts are highlighted in the same color.

Strand name	Sequence (5'→'3')
J1	GGATCAGAGCTGGACG ACAATGACGTAGGTCC TTTT GGACCTACGTCATTGT ACTATGGCACACATCC
J2	GCAAGACTCGTGCTCA CCGAATGCCACCACGC TTTT GCGTGGTGGCATTCGG CGTCCAGCTCTGATCC
J3	GGTTCAGCCGCAATCC TCGCCTGCACTCTACC TTTT GGTAGAGTGCAGGCGA TGAGCACGAGTCTTGC
J4a	TACTGCGCTTCGAT TT GGATGTGTGCCATAGT GGATTGCGGCTGAACC
J4b	AACTGAGGGAGCCT TT GGATGTGTGCCATAGT GGATTGCGGCTGAACC
J4c	AGACTAATTCTCCT TT GGATGTGTGCCATAGT GGATTGCGGCTGAACC

Supplementary Table S2. DNA scaffold complementary oligonucleotides

Oligo number	Sequence (5'→'3')
1	TTTTCGTAATCATGGTCATAGCTGTTTCCTGTGTGAAATTGTTATC
2	CGCTCACAATTCCACACAACATACGAGCCGGAAGCATA
3	AAGTGTAAAGCCTGGGGTGCCTAATGAGTGAGCTAACT
4	CACATTAATTGCGTTGCGCTCACTGCCCGCTTTCCAGT
5	CGGGAAACCTGTCGTGCCAGCTGCATTAATGAATCGGC
6	CAACGCGCGGGGAGAGGCGGTTTGCGTATTGGGCGCCA
7	GGGTGGTTTTTCTTTTCACCAGTGAGACGGGCAACAGC
8	TGATTGCCCTTCACCGCCTGGCCCTGAGAGAGTTGCAG
9	CAAGCGGTCCACGCTGGTTTGCCCCAGCAGGCGAAAAT
10	CCTGTTTGATGGTGGTTCCGAAATCGGCAAAATCCCTT
11	ATAAATCAAAAGAATAGCCCGAGATAGGGTTGAGTGTT
12	GTTCCAGTTTGGAACAAGAGTCCACTATTAAAGAACGT
13	GGACTCCAACGTCAAAGGGCGAAAAACCGTCTATCAGG
14	GCGATGGCCCACTACGTGAACCATCACCCAAATCAAGT
15	TTTTTGGGGTCGAGGTGCCGTAAAGCACTAAATCGGAA
16	CCCTAAAGGGAGCCCCCGATTTAGAGCTTGACGGGGAA
17	AGCCGGCGAACGTGGCGAGAAAGGAAGGGAAGAAAGCG
18	AAAGGAGCGGGCGCTAGGGCGCTGGCAAGTGTAGCGGT
19	CACGCTGCGCGTAACCACCACACCCGCCGCGCTTAATG
20	CGCCGCTACAGGGCGCGTACTATGGTTGCTTTGACGAG
21	CACGTATAACGTGCTTTCCTCGTTAGAATCAGAGCGGG
22	AGCTAAACAGGAGGCCGATTAAAGGGATTTTAGACAGG
23	AACGGTACGCCAGAATCCTGAGAAGTGTTTTTATAATC
24	AGTGAGGCCACCGAGTAAAAGAGTCTGTCCATCACGCA
25	AATTAACCGTTGTAGCAATACTTCTTTGATTAGTAATA
26	ACATCACTTGCCTGAGTAGAAGAACTCAAACTATCGGC
27	CTTGCTGGTAATATCCAGAACAATATTACCGCCAGCCA
28	TTGCAACAGGAAAAACGCTCATGGAAATACCTACATTT
29	TGACGCTCAATCGTCTGAAATGGATTATTTACATTGGC
30	AGATTCACCAGTCACACGACCAGTAATAAAAGGGACAT
31	TCTGGCCAACAGAGATAGAACCCTTCTGACCTGAAAGC
32	GTAAGAATACGTGGCACAGACAATATTTTTGAATGGCT
33	ATTAGTCTTTAATGCGCGAACTGATAGCCCTAAAACAT
34	CGCCATTAAAAATACCGAACGAACCACCAGCAGAAGAT
35	AAAACAGAGGTGAGGCGGTCAGTATTAACACCGCCTGC
36	AACAGTGCCACGCTGAGAGCCAGCAGCAAATGAAAAAT
37	CTAAAGCATCACCTTGCTGAACCTCAAATATCAAACCC
38	TCAATCAATATCTGGTCAGTTGGCAAATCAACAGTTGA
39	AAGGAATTGAGGAAGGTTATCTAAAATATCTTTAGGAG
40	CACTAACAACTAATAGATTAGAGCCGTCAATAGATAAT
41	ACATTTGAGGATTTAGAAGTATTAGACTTTACAAACAA

42	TTCGACAACTCGTATTAAATCCTTTGCCCGAACGTTAT
43	TAATTTTAAAAGTTTGAGTAACATTATCATTTTGCGGA
44	ACAAAGAAACCACCAGAAGGAGCGGAATTATCATCATA
45	TTCCTGATTATCAGATGATGGCAATTCATCAATATAAT
46	CCTGATTGTTTGGATTATACTTCTGAATAATGGAAGGG
47	TTAGAACCTACCATATCAAAATTATTTGCACGTAAAAC
48	AGAAATAAAGAAATTGCGTAGATTTTCAGGTTTAACGT
49	CAGATGAATATACAGTAACAGTACCTTTTACATCGGGA
50	GAAACAATAACGGATTCGCCTGATTGCTTTGAATACCA
51	AGTTACAAAATCGCGCAGAGGCGAATTATTCATTTCAA
52	TTACCTGAGCAAAAGAAGATGATGAAACAAACATCAAG
53	AAAACAAAATTAATTACATTTAACAATTTCATTTGAAT
54	TACCTTTTTTAATGGAAACAGTACATAAATCAATATAT
55	GTGAGTGAATAACCTTGCTTCTGTAAATCGTCGCTATT
56	AATTAATTTTCCCTTAGAATCCTTGAAAACATAGCGAT
57	AGCTTAGATTAAGACGCTGAGAAGAGTCAATAGTGAAT
58	TTATCAAAATCATAGGTCTGAGAGACTACCTTTTTAAC
59	CTCCGGCTTAGGTTGGGTTATATAACTATATGTAAATG
60	CTGATGCAAATCCAATCGCAAGACAAAGAACGCGAGAA
61	AACTTTTTCAAATATATTTTAGTTAATTTCATCTTCTG
62	ACCTAAATTTAATGGTTTGAAATACCGACCGTGTGATA
63	AATAAGGCGTTAAATAAGAATAAACACCGGAATCATAA
64	TTACTAGAAAAAGCCTGTTTAGTATCATATGCGTTATA
65	CAAATTCTTACCAGTATAAAGCCAACGCTCAACAGTAG
66	GGCTTAATTGAGAATCGCCATATTTAACAACGCCAACA
67	TGTAATTTAGGCAGAGGCATTTTCGAGCCAGTAATAAG
68	AGAATATAAAGTACCGACAAAAGGTAAAGTAATTCTGT
69	CCAGACGACGACAATAAACAACATGTTCAGCTAATGCA
70	GAACGCGCCTGTTTATCAACAATAGATAAGTCCTGAAC
71	AAGAAAAATAATATCCCATCCTAATTTACGAGCATGTA
72	GAAACCAATCAATAATCGGCTGTCTTTCCTTATCATTC
73	CAAGAACGGGTATTAAACCAAGTACCGCACTCATCGAG
74	AACAAGCAAGCCGTTTTTATTTTCATCGTAGGAATCAT
75	TACCGCGCCCAATAGCAAGCAAATCAGATATAGAAGGC
76	TTATCCGGTATTCTAAGAACGCGAGGCGTTTTAGCGAA
77	CCTCCCGACTTGCGGGAGGTTTTGAAGCCTTAAATCAA
78	GATTAGTTGCTATTTTGCACCCAGCTACAATTTTATCC
79	TGAATCTTACCAACGCTAACGAGCGTCTTTCCAGAGCC
80	TAATTTGCCAGTTACAAAATAAACAGCCATATTATTTA
81	TCCCAATCCAAATAAGAAACGATTTTTTGTTTAACGTC
82	AAAAATGAAAATAGCAGCCTTTACAGAGAGAATAACAT
83	AAAAACAGGGAAGCGCATTAGACGGGAGAATTAACTGA
84	ACACCCTGAACAAAGTCAGAGGGTAATTGAGCGCTAAT
85	ATCAGAGAGATAACCCACAAGAATTGAGTTAAGCCCAA
86	TAATAAGAGCAAGAAACAATGAAATAGCAATAGCTATC

87	TTACCGAAGCCCTTTTTAAGAAAAGTAAGCAGATAGCC
88	GAACAAAGTTACCAGAAGGAAACCGAGGAAACGCAATA
89	ATAACGGAATACCCAAAAGAACTGGCATGATTAAGACT
90	CCTTATTACGCAGTATGTTAGCAAACGTAGAAAATACA
91	TACATAAAGGTGGCAACATATAAAAGAAACGCAAAGAC
92	ACCACGGAATAAGTTTATTTTGTCACAATCAATAGAAA
93	ATTCATATGGTTTACCAGCGCCAAAGACAAAAGGGCGA
94	CATTCAACCGATTGAGGGAGGGAAGGTAAATATTGACG
95	GAAATTATTCATTAAAGGTGAATTATCACCGTCACCGA
96	CTTGAGCCATTTGGGAATTAGAGCCAGCAAAATCACCA
97	GTAGCACCATTACCATTAGCAAGGCCGGAAACGTCACC
98	AATGAAACCATCGATAGCAGCACCGTAATCAGTAGCGA
99	CAGAATCAAGTTTGCCTTTAGCGTCAGACTGTAGCGCG
100	TTTTCATCGGCATTTTCGGTCATAGCCCCCTTATTAGC
101	GTTTGCCATCTTTTCATAATCAAAATCACCGGAACCAG
102	AGCCACCACCGGAACCGCCTCCCTCAGAGCCGCCACCC
103	TCAGAACCGCCACCCTCAGAGCCACCACCCTCAGAGCC
104	GCCACCAGAACCACCACCAGAGCCGCCGCCAGCATTGA
105	CAGGAGGTTGAGGCAGGTCAGACGATTGGCCTTGATAT
106	TCACAAACAAATAAATCCTCATTAAAGCCAGAATGGAA
107	AGCGCAGTCTCTGAATTTACCGTTCCAGTAAGCGTCAT
108	ACATGGCTTTTGATGATACAGGAGTGTACTGGTAATAA
109	GTTTTAACGGGGTCAGTGCCTTGAGTAACAGTGCCCGT
110	ATAAACAGTTAATGCCCCCTGCCTATTTCGGAACCTAT
111	TATTCTGAAACATGAAAGTATTAAGAGGCTGAGACTCC
112	TCAAGAGAAGGATTAGGATTAGCGGGGTTTTGCTCAGT
113	ACCAGGCGGATAAGTGCCGTCGAGAGGGTTGATATAAG
114	TATAGCCCGGAATAGGTGTATCACCGTACTCAGGAGGT
115	TTAGTACCGCCACCCTCAGAACCGCCACCCTCAGAACC
116	GCCACCCTCAGAGCCACCACCCTCATTTTCAGGGATAG
117	CAAGCCCAATAGGAACCCATGTACCGTAACACTGAGTT
118	TCGTCACCAGTACAAACTACAACGCCTGTAGCATTCCA
119	CAGACAGCCCTCATAGTTAGCGTAACGATCTAAAGTTT
120	TGTCGTCTTTCCAGACGTTAGTAAATGAATTTTCTGTA
121	TGGGATTTTGCTAAACAACTTTCAACAGTTTCAGCGGA
122	GTGAGAATAGAAAGGAACAACTAAAGGAATTGCGAATA
123	ATAATTTTTTCACGTTGAAAATCTCCAAAAAAAAGGCT
124	CCAAAAGGAGCCTTTAATTGTATCGGTTTATCAGCTTG
125	CTTTCGAGGTGAATTTCTTAAACAGCTTGATACCGATA
126	GTTGCGCCGACAATGACAACAACCATCGCCCACGCATA
127	ACCGATATATTCGGTCGCTGAGGCTTGCAGGGAGTTAA
128	AGGCCGCTTTTGCGGGATCGTCACCCTCAGCAGCGAAA
129	GACAGCATCGGAACGAGGGTAGCAACGGCTACAGAGGC
130	TTTGAGGACTAAAGACTTTTTCATGAGGAAGTTTCCAT
131	TAAACGGGTAAAATACGTAATGCCACTACGAAGGCACC

132	AACCTAAAACGAAAGAGGCAAAAGAATACACTAAAACA
133	CTCATCTTTGACCCCCAGCGATTATACCAAGCGCGAAA
134	CAAAGTACAACGGAGATTTGTATCATCGCCTGATAAAT
135	TGTGTCGAAATCCGCGACCTGCTCCATGTTACTTAGCC
136	GGAACGAGGCGCAGACGGTCAATCATAAGGGAACCGAA
137	CTGACCAACTTTGAAAGAGGACAGATGAACGGTGTACA
138	GACCAGGCGCATAGGCTGGCTGACCTTCATCAAGAGTA
139	ATCTTGACAAGAACCGGATATTCATTACCCAAATCAAC
140	GTAACAAAGCTGCTCATTCAGTGAATAAGGCTTGCCCT
141	GACGAGAAACACCAGAACGAGTAGTAAATTGGGCTTGA
142	GATGGTTTAATTTCAACTTTAATCATTGTGAATTACCT
143	TATGCGATTTTAAGAACTGGCTCATTATACCAGTCAGG
144	ACGTTGGGAAGAAAAATCTACGTTAATAAAACGAACTA
145	ACGGAACAACATTATTACAGGTAGAAAGATTCATCAGT
146	TGAGATTTAGGAATACCACATTCAACTAATGCAGATAC
147	ATAACGCCAAAAGGAATTACGAGGCATAGTAAGAGCAA
148	CACTATCATAACCCTCGTTTACCAGACGACGATAAAAA
149	CCAAAATAGCGAGAGGCTTTTGCAAAAGAAGTTTTGCC
150	AGAGGGGGTAATAGTAAAATGTTTAGACTGGATAGCGT
151	CCAATACTGCGGAATCGTCATAAATATTCATTGAATCC
152	CCCTCAAATGCTTTAAACAGTTCAGAAAACGAGAATGA
153	CCATAAATCAAAAATCAGGTCTTTACCCTGACTATTAT
154	AGTCAGAAGCAAAGCGGATTGCATCAAAAAGATTAAGA
155	GGAAGCCCGAAAGACTTCAAATATCGCGTTTTAATTCG
156	AGCTTCAAAGCGAACCAGACCGGAAGCAAACTCCAACA
157	GGTCAGGATTAGAGAGTACCTTTAATTGCTCCTTTTGA
158	TAAGAGGTCATTTTTGCGGATGGCTTAGAGCTTAATTG
159	CTGAATATAATGCTGTAGCTCAACATGTTTTAAATATG
160	CAACTAAAGTACGGTGTCTGGAAGTTTCATTCCATATA
161	ACAGTTGATTCCCAATTCTGCGAACGAGTAGATTTAGT
162	TTGACCATTAGATACATTTCGCAAATGGTCAATAACCT
163	GTTTAGCTATATTTTCATTTGGGGCGCGAGCTGAAAAG
164	GTGGCATCAATTCTACTAATAGTAGTAGCATTAACATC
165	CAATAAATCATACAGGCAAGGCAAAGAATTAGCAAAAT
166	TAAGCAATAAAGCCTCAGAGCATAAAGCTAAATCGGTT
167	GTACCAAAAACATTATGACCCTGTAATACTTTTGCGGG
168	AGAAGCCTTTATTTCAACGCAAGGATAAAAATTTTTAG
169	AACCCTCATATATTTTAAATGCAATGCCTGAGTAATGT
170	GTAGGTAAAGATTCAAAAGGGTGAGAAAGGCCGGAGAC
171	AGTCAAATCACCATCAATATGATATTCAACCGTTCTAG
172	CTGATAAATTAATGCCGGAGAGGGTAGCTATTTTTGAG
173	AGATCTACAAAGGCTATCAGGTCATTGCCTGAGAGTCT
174	GGAGCAAACAAGAGAATCGATGAACGGTAATCGTAAAA
175	CTAGCATGTCAATCATATGTACCCCGGTTGATAATCAG
176	AAAAGCCCCAAAAACAGGAAGATTGTATAAGCAAATAT

177	TTAAATTGTAAACGTTAATATTTTGTTAAAATTCGCAT
178	TAAATTTTTGTTAAATCAGCTCATTTTTTAACCAATAG
179	GAACGCCATCAAAAATAATTCGCGTCTGGCCTTCCTGT
180	AGCCAGCTTTCATCAACATTAAATGTGAGCGAGTAACA
181	ACCCGTCGGATTCTCCGTGGGAACAAACGGCGGATTGA
182	CCGTAATGGGATAGGTCACGTTGGTGTAGATGGGCGCA
183	TCGTAACCGTGCATCTGCCAGTTTGAGGGGACGACGAC
184	AGTATCGGCCTCAGGAAGATCGCACTCCAGCCAGCTTT
185	CCGGCACCGCTTCTGGTGCCGGAAACCAGGCAAAGCGC
186	CATTCGCCATTCAGGCTGCGCAACTGTTGGGAAGGGCG
187	ATCGGTGCGGGCCTCTTCGCTATTACGCCAGCTGGCGA
188	AAGGGGGATGTGCTGCAAGGCGATTAAGTTGGGTAACG
189	CCAGGGTTTTCCCAGTCACGACGTTGTAAAACGACGGC
190	CAGTGCCAAGCTTGCATGCCTGCAGGTCGACTCTAGAGGATCTTTT

Supplementary Table S3. Oligonucleotides were replaced from Table S2 to assemble reference structures. The DNA dumbbell forming sequence is indicated in red.

Name	Sequence (5' → 3')	Length (nt)	# of oligos replaced
REF 1.1	ACATCACTTGCCTGAGTAGA	20	
REF 1.2	AGAACTCAAATCCTCTTTTGAGGAACAAGTTTTCTTGTCTATCGGCCT	48	
REF 1.3	TGCTGGTAATTCCTCTTTTGAGGAACAAGTTTTCTTGTATCCAGAACA	48	
REF 1.4	ATATTACCGCTCCTCTTTTGAGGAACAAGTTTTCTTGTCAGCCATTGC	48	
REF 1.5	AACAGGAAAATCCTCTTTTGAGGAACAAGTTTTCTTGTACGCTCATGG	48	26-30
REF 1.6	AAATACCTACTCCTCTTTTGAGGAACAAGTTTTCTTGTATTTTGACGC	48	
REF 1.7	TCAATCGTCTTCCTCTTTTGAGGAACAAGTTTTCTTGTGAAATGGATT	48	
REF 1.8	ATTTACATTGGCAGATTCAC	20	
REF 1.9	CAGTCACACGACCAGTAATAAAAGGGACAT	30	
REF 2.1	TCACAAACAAATAAATCCTCATTAAAGCCAGAATGGAAAGCGCAGTCTCTGAATTT	56	
REF 2.2	ACCGTTCCAGTAAGCGTCAT	20	
REF 2.3	ACATGGCTTTTCCTCTTTTGAGGAACAAGTTTTCTTGTTGATGATACA	48	
REF 2.4	GGAGTGTACTTCCTCTTTTGAGGAACAAGTTTTCTTGTGGTAATAAGT	48	
REF 2.5	TTTAACGGGGTCCTCTTTTGAGGAACAAGTTTTCTTGTTCAGTGCCTT	48	106-112
REF 2.6	GAGTAACAGTTCCTCTTTTGAGGAACAAGTTTTCTTGTGCCCGTATAA	48	
REF 2.7	ACAGTTAATGTCCTCTTTTGAGGAACAAGTTTTCTTGTCCCCCTGCCT	48	
REF 2.8	ATTTCGGAACTCCTCTTTTGAGGAACAAGTTTTCTTGTCTATTATTCT	48	

REF 2.9	GAAACATGAAAGTATTAAGA	20
REF 2.10	GGCTGAGACTCCTCAAGAGAAGGATTAGGATTAGCGGG GTTTTGCTCAGT	50

Section S4. AFM imaging

Section 4.1 AFM imaging

Atomic Force Microscopy (Nanosurf Mobile S) imaging of nanobaits was performed in the air in a non-contact mode. All scans were performed on a bare mica surface following the adsorption of nanobaits as follows. We placed a 10 μL drop of a DNA solution (diluted to 1 ng/μL in filtered 10 mM $MgCl_2$ and 10 mM Tris-HCl, pH 8.0) onto a freshly cleaved mica surface for 1 minute, rinsed the mica plate three times with 100 μL of Mili-Q water and then blow-dried it with Nitrogen. Before the scan, the mica plate was affixed to the AFM sample stage using double-sided adhesive tape. Image visualization and analysis were done using Gwyddion.

Section 4.2 AFM images of nanobait

AFM images of nanobait are shown in Figures S3 and S4. Figure S3a presents AFM images of nanobait structure without any label added. In some cases, two references are visible (circled in dark grey, Figure S3a, right). However, it is known that DNA dumbbell structures are hardly distinguishable with AFM imaging in comparison to nanopores [3].

Nanobait events with monovalent streptavidin (Figure S3b) indicate five structures that correspond to capture sites with labels, as expected from the nanobait design. The same design but with the DNA flower label is presented in Figure S4. The DNA flower is larger than streptavidin and hence is easier to be detected with the AFM imaging (Figure S1).

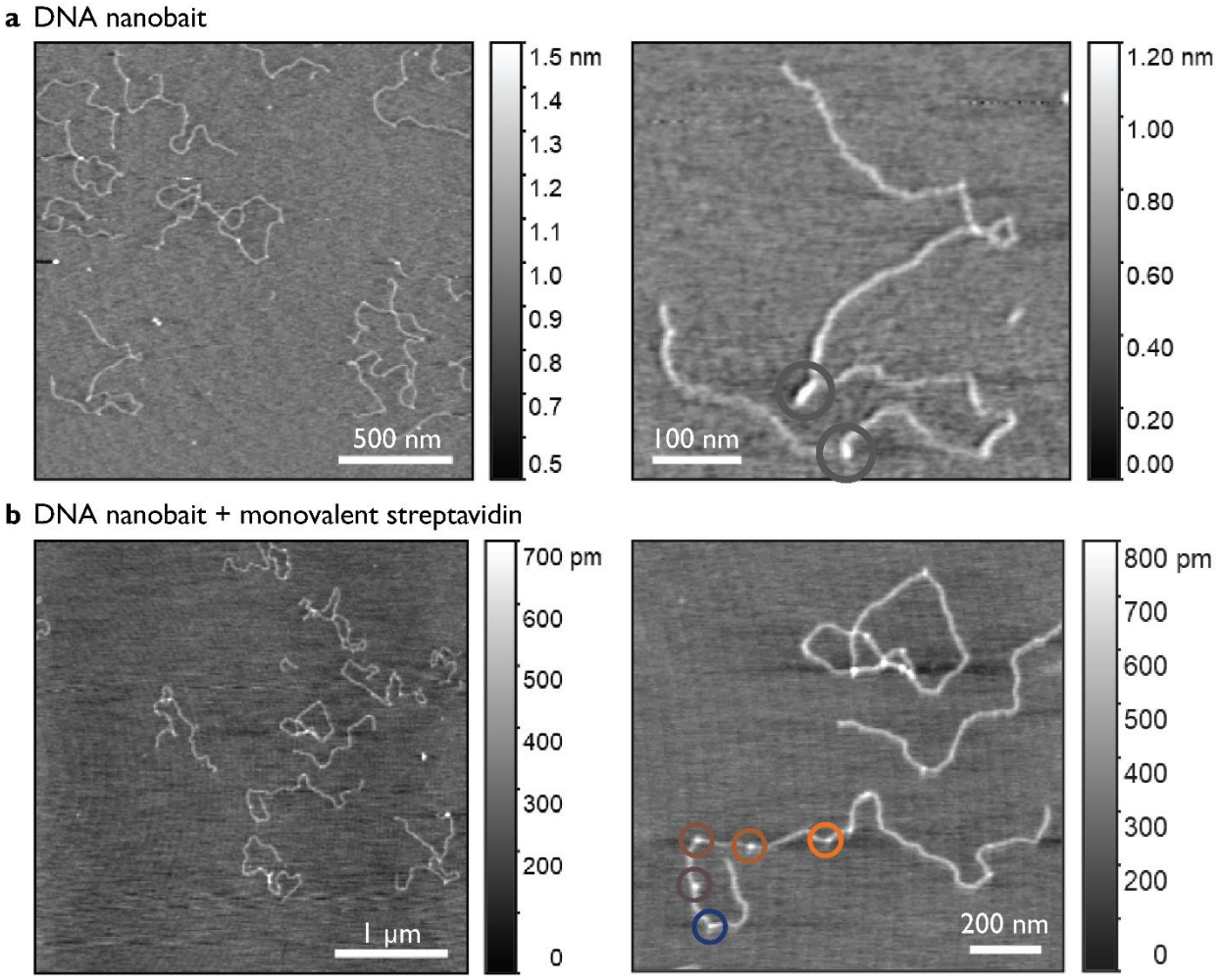

Figure S3. AFM images of DNA nanobait. a) Nanobait without monovalent streptavidin have two reference structures (circled in dark grey). b) AFM images of nanobait with monovalent streptavidin used as a label. Five capture sites are circled in corresponding colors.

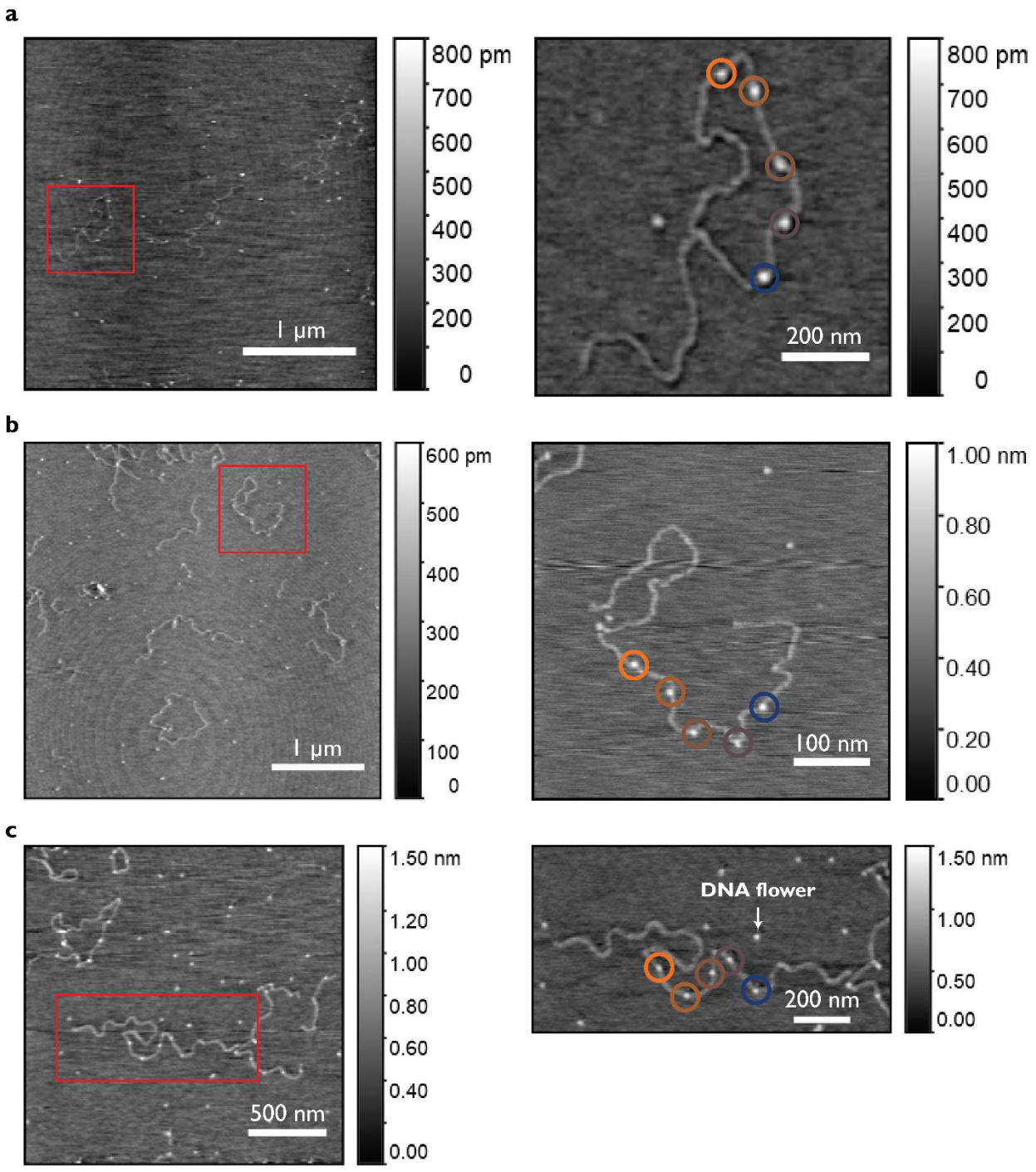

Figure S4. AFM images of nanobait with DNA flower as a label. Three different nanobait example images are shown in a), b), and c).

Section S5. EMSA analysis

We performed electrophoretic mobility shift assay (EMSA) to see a gel shift caused by streptavidin binding to all five sites on nanobait (Figure S5). 2 % (w/v) agarose (BioReagent, low electroendosmosis, Merck SigmaAldrich; catalog number A9539) gel was prepared by adding 2 g of agarose, 10 mL of 10 × Tris-Borate-EDTA buffer (TBE buffer), and Milli-Q water was added to 100 mL. The gel was heated in the microwave at the maximum power (800 W) for 2-3 min. It was cooled down and poured into a gel tray for 45 min.

Samples were mixed with purple gel loading dye (New England Biolabs; catalog number B7025S) and TBE buffer to 1 × with ~150 ng of a DNA sample. We used a 1 kb DNA ladder as a reference (New England Biolabs; catalog number N3232) with a size range from 500 bp to 10 kb (Figure S5a). nanobait in lane 2 (Figure S5a) was mixed with 10 × excess of wild-type tetravalent streptavidin (ThermoFisher Scientific; catalog number 21125).

It can be observed from the agarose gel in Figure S5a that there is a slight shift from nanobait (lane 1) to nanobait + streptavidin (lane 2). We used gel intensity analysis using an open-source software Fiji[8] to plot this shift, indicating that streptavidin(s) is bound to nanobait (Figure S5b).

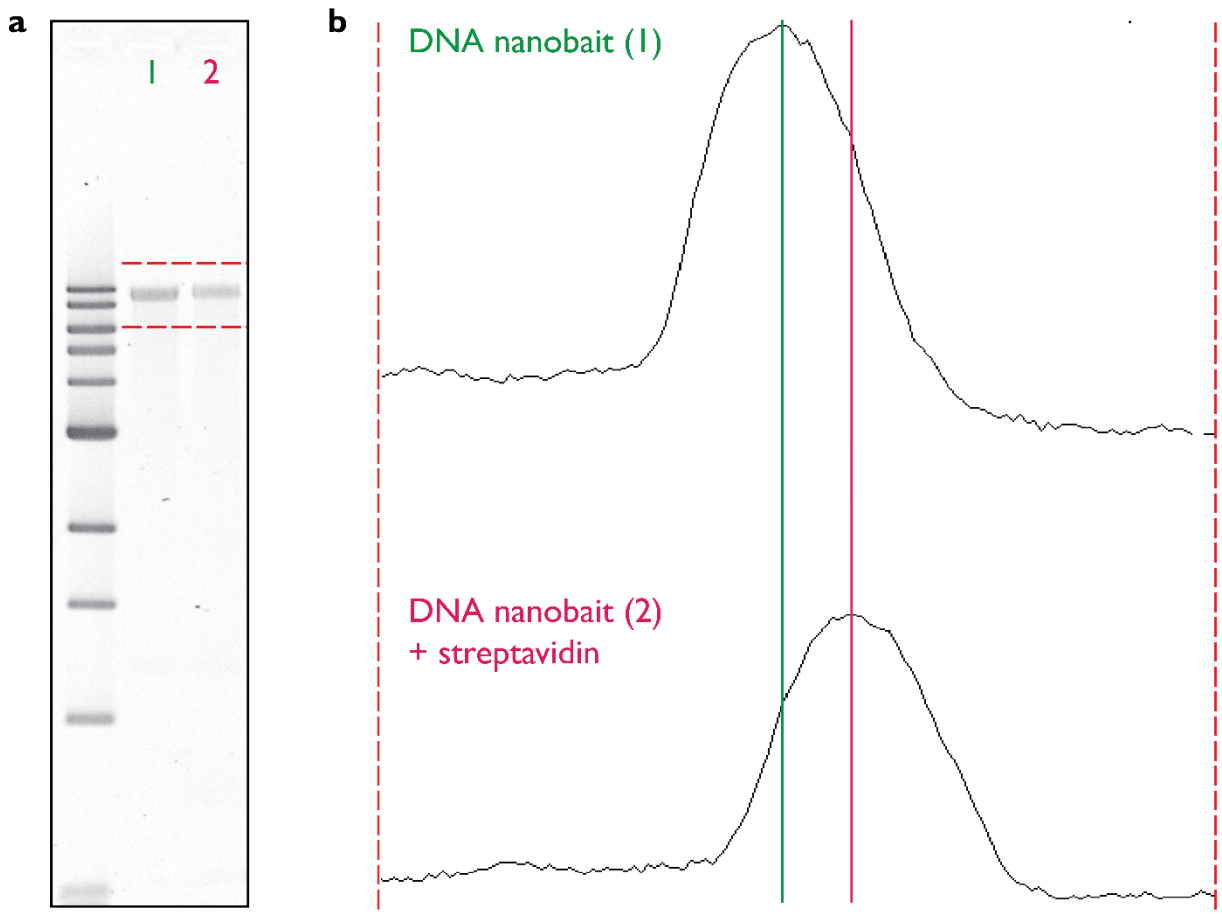

Figure S5. Electrophoretic mobility shift assay (EMSA) of nanobait without and with streptavidin. a) 2% (w/v) agarose gel od nanobait without (lane 1) and with (lane 2) streptavidin added. We used a 1 kb DNA ladder (New England Biolabs; product number N3232). The two top lines of the ladder have 10 and 8 kb. b) The intensity traces of corresponding lanes from a). The green line indicates the peak of nanobait (lane 1) and the peak of nanobait + streptavidin (lane 2). The shift between the green and purple lines corresponds to streptavidin(s) bound to capture sites on nanobait.

Section S6. Multiple respiratory viruses DNA nanobait sequences and example events

Nanobait for multiple respiratory viruses is prepared as previously described in Section S2. Below, are listed sequences of capture sites (Table S6), biotin strand (Table S5), and target sequence (Table S4) for each virus.

We also show here additional nanopore events of nanobait without target added (Figure S6a), with SARS-CoV-2 target (Figure S6b), Influenza A (Figure S6c), RSV (Figure S6d), Parainfluenza (Figure S6e), and Rhinoviruses (Figure S6f). Targets for Influenza A, Parainfluenza A, and Rhinoviruses target a group of those viruses rather than a single variant [9,10]. The nananobait and peaks resemble those presented in Figure 2a of the manuscript. These single-molecule events are obtained from three nanopore measurements.

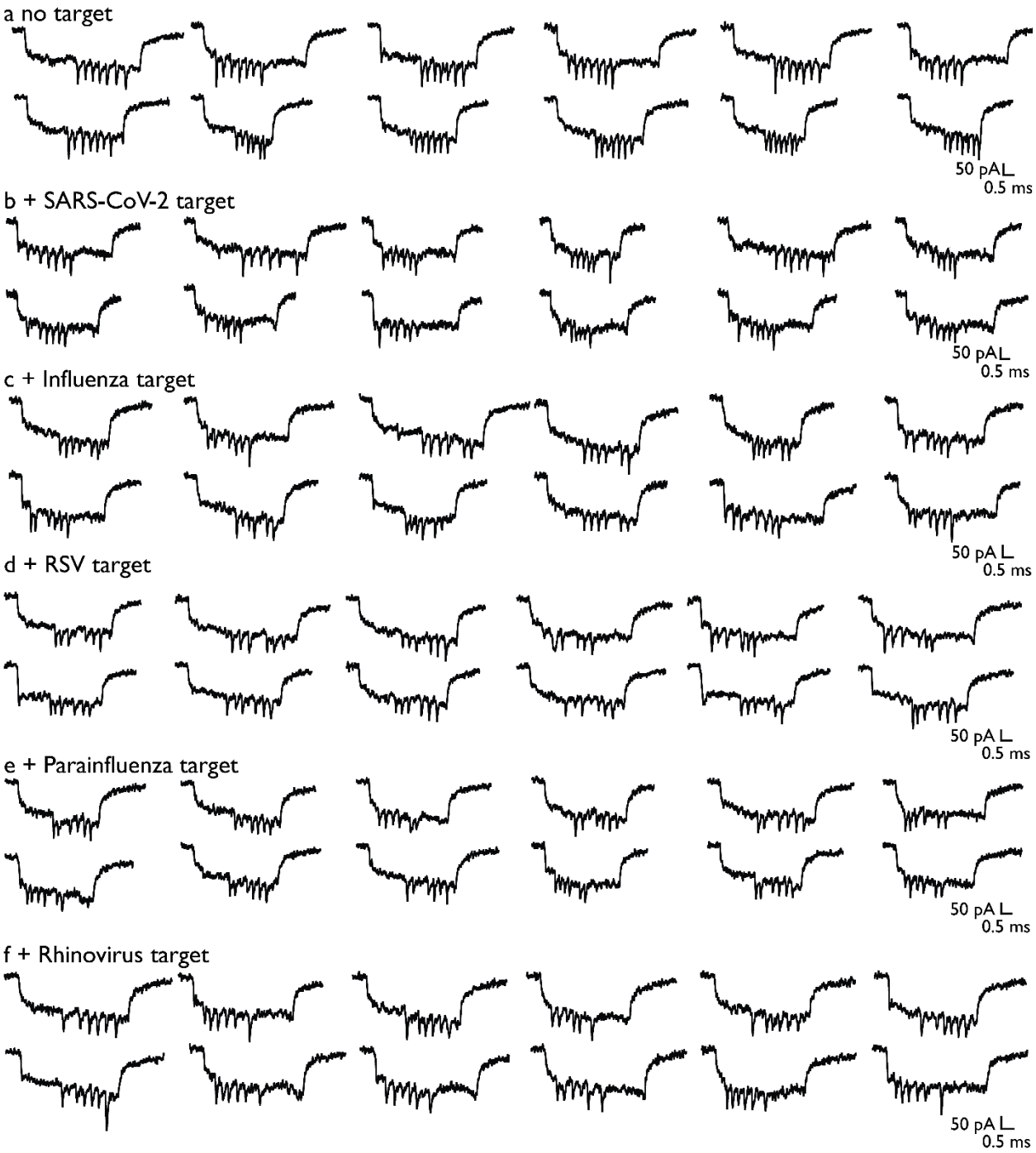

Figure S6. Additional example events for nanobait used for identification of various respiratory viruses with a) no target added, b) SARS-CoV-2 target, c) Influenza target, d) RSV, e) Parainfluenza target, and f) Rhinovirus target.

Supplementary Table S4. Presence of peaks at their respective sites for the multiple virus identification.

Target/Case	Control (no targets)	Standard error	Target present	Standard error
SARS-CoV-2	0.17	0.04	0.75	0.10
RSV	0.09	0.01	0.96	0.06
Rhinovirus	0.08	0.03	0.89	0.13
Influenza	0.11	0.04	0.49	0.17
Parainfluenza	0.03	0.01	0.73	0.04

Supplementary Table S5. Target sequences for the multiple virus identification.

Strand name	Virus / group of viruses	Sequence reference	Sequence (5' → 3')
SW	SARS-CoV-2_Wuhan	NCBI Reference Sequence: NC_045512.2[11]	GTATGAAAATGCCTTTTTAC
Infl	Influenza A viruses universal	Sequence adapted from[12]	TGACAGGATTGGTCTTGTCT
RSV	Respiratory syncytial virus universal A	Sequence adapted from[13]	ACACAGCAGCTGTTCAGTAC
PI	Parainfluenza 1	Sequence adapted from[10]	CTTCCTGCTGGTGTGTTAAT
RV	Rhinoviruses universal	Sequence adapted from[9]	TCCTCCGGCCCCTGAATGTG

Supplementary Table S6. 3' biotinylated strand sequences for the multiple virus identification.

Strand name	Virus / group of viruses	Sequence (5' → 3')
bSW	SARS-CoV-2_Wuhan	AAATGCCTTTTTAC/3-biotin/
bInfl	Influenza A viruses universal	GATTGGTCTTGTCT/3-biotin/
bRSV	Respiratory syncytial virus universal A	CAGCTGTTCAGTAC/3-biotin/
bPI	Parainfluenza 1	GCTGGTGTGTTAAT/3-biotin/

bRV	Rhinoviruses universal	GGCCCCTGAATGTG /3-biotin/

Supplementary Table S7. Capture strand sequences for multiple virus identification.

Strand name	Virus / group of viruses	Sequence (5' → 3')
cSW_42	SARS-CoV-2_Wuhan	TTCGACAACTCGTATTAAATCCTTTGCCCGAACGTTAT TTTTT GTAAAAAGGCATTTTCATAC
cRSV_55	Respiratory syncytial virus universal A	GTGAGTGAATAACCTTGCTTCTGTAAATCGTCGCTATT TTTTT GTACTGAACAGCTGCTGTGT
cRV_68	Rhinoviruses universal	AGAATATAAAGTACCGACAAAAGGTAAAGTAATTCTGT TTTTT CACATTCAGGGGCCGGAGGA
cI_81	Influenza A viruses universal	TCCCAATCCAAATAAGAAACGATTTTTTGTTTAACGTC TTTTT AGACAAGACCAATCCTGTCA
cPI_94	Parainfluenza 1	CATTCAACCGATTGAGGGAGGGAAGGTAAATATTGACG TTTTT ATTAACACACCAGCAGGAAG

Section S7. Multiple SARS-Co-V-2 virus variants DNA nanobait sequences and example events

Nanobait for multiple SARS-CoV-2 variants is prepared as previously described in Section S2. Below, are listed sequences of capture sites (Table S10), biotin strand (Table S8), and target sequence wildtype (Table S9) and variant (Table S7) for each virus.

We also show here additional nanopore events of nanobait without target added (Figure S7a), with B reference target (Figure S7b), B.1.617 variant target (Figure S7c), B.1 variant target (Figure S7d), B.1.1.7 variant target (Figure S7e), and B.1.351 variant target (Figure S7f). The nanobait and peaks resemble those presented in Figure 2b of the manuscript. These single-molecule events are obtained from three nanopore measurements.

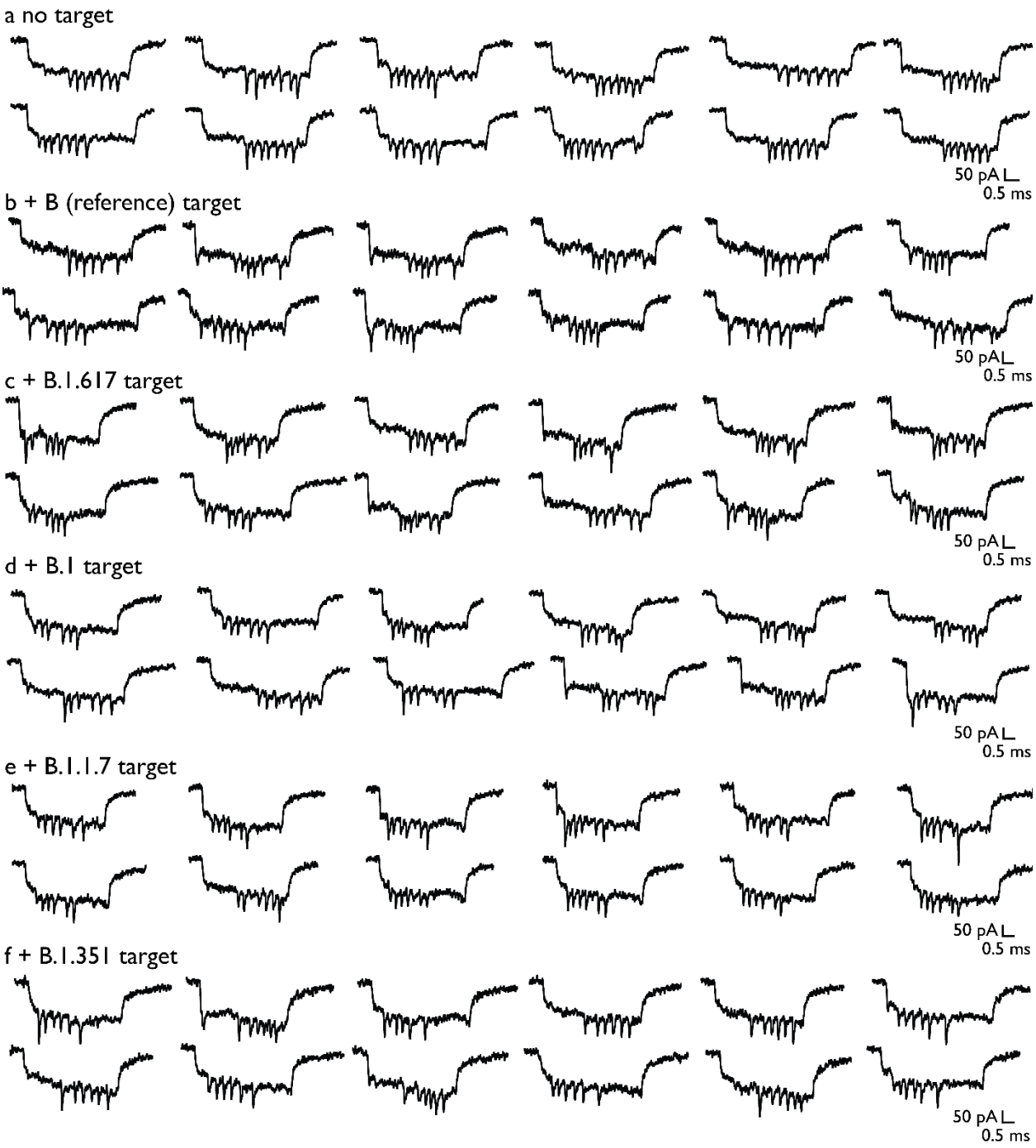

Figure S7. Additional example events for nanobait used for identification of various SARS-CoV-2 variants with a) no target added, b) B target, c) B.1.617 variant target, d) B.1 variant target, e) B.1.1.7 variant target, and f) B.1.351 variant target.

Supplementary Table S8. Presence of peaks at their respective sites for the multiple variant identification.

Target/Case	Control (no targets)	Standard error	WT target present	Standard error	Variant target present	Standard error
B (Wuhan)	0.08	0.00	0.93	0.04	0.92	0.06
B.1.617 (Indian)	0.23	0.01	0.39	0.02	0.77	0.01
B.1 (European)	0.02	0.00	0.29	0.05	0.98	0.06
B.1.1.7 (British)	0.04	0.00	0.06	0.02	0.96	0.12
B.1.351 (South African)	0.10	0.00	0.49	0.11	0.90	0.03

Supplementary Table S9. Target sequences for the multiple SARS-CoV-2 variant identification. In red, single nucleotide variant positions are highlighted, while yellow highlights the toehold region used for the strand displacement reaction.

Strandname	WHO nomenclature[14]	Pangolin nomenclature[15]	Single nucleotide variation	Sequence (5' → 3')
SW	Reference	B (reference)	/	GTATGAAAATGCCTTTTTAC
SIm	Delta	B.1.617 (Indian)	T-G L452R	CCGGTATAGATTGTTTAGGA
SEm	NA	B.1 (European)	A-G D614G	GGTGTTAACTGCACAGAAGT
SUKm	Alpha	B.1.1.7 (British)	A-T N501Y	CTTATGGTGTTGGTTACCAA
SSAm	Beta	B.1.351 (South African)	G-A E484K	TAAAGGTTTTAATTGTTACT

Supplementary Table S10. 3' biotinylated strand sequences for the multiple SARS-CoV-2 variant identification.

Strand name	Variant name	Sequence (5’ → 3’)
bSW	B (reference)	AAATGCCTTTTTAC/3-BIOTIN/
bSIm	B.1.617 (Indian)	TAGATTGTTTAGGA/3-BIOTIN/
bSEm	B.1 (European)	AACTGCACAGAAGT/3-BIOTIN/
bSUKm	B.1.1.7 (British)	GTGTTGGTTACCAA/3-BIOTIN/
bSSAm	B.1.351 (South African)	TTTTAATTGTTACT/3-BIOTIN/

Supplementary Table S11. Wild-type (WT) target sequences for the multiple SARS-CoV-2 variant identification. In green, wild-type nucleotide positions are highlighted, while yellow highlights the toehold region used for the strand displacement reaction.

Strand name	Sequence (5’ → 3’)	Length (nt)
SI	CCTGTATAGATTGTTTAGGA	20
SE	GATGTTAACTGCACAGAAGT	20
SUK	CTAATGGTGTTGGTTACCAA	20
SSA	TGAAGGTTTTAATTGTTACT	20

Supplementary Table S12. Capture strand sequences for the multiple SARS-CoV-2 variant identification.

Strand name	Variant name	Sequence (5’ → 3’)
cSW_42	B (reference)	TTCGACAACTCGTATTAAATCCTTTGCCCGAACGTTAT TTTTT GTAAAAAGGCATTTTCATAC
cSI_68	B.1.617 (Indian)	AGAATATAAAGTACCGACAAAAGGTAAAGTAATTCTGT TTTTT TCCTAAACAATCTATACCGG
cSE_94	B.1 (European)	CATTCAACCGATTGAGGGAGGGAAGGTAAATATTGACG TTTTT ACTTCTGTGCAGTTAACACC
cSUK_81	B.1.1.7 (British)	TCCCAATCCAAATAAGAAACGATTTTTTGTTTAACGTC TTTTT TTGGTAACCAACACCATAAG

cSSA_55	B.1.351 (South African)	GTGAGTGAATAACCTTGCTTCTGTAAATCGTCGCTATT TTTTT AGTAACAATTAAAACCTTTA

Section S8. Kinetics of strand displacement reaction with DNA and RNA targets

Nanobait for multiple SARS-CoV-2 targets is prepared as previously described in Section S2. Below, are listed sequences of capture sites (Table S13), biotin strands (Table S12), and target strands (Table S11).

Kinetics measurements for all five targets SDR are shown in Figure S8 and fifty nanobait events are analyzed per each data point. We tested targets of the same sequence but with different backbones as RNAs or DNAs (Figure S8a and S8b, respectively). Here, we show that target chemistry might have effects on the kinetics of the SDR since some of the targets (e.g. target 3) have slower SDR for RNA sequence than for DNA sequence.

We also show here additional nanopore events of nanobait without target added (Figure S8c) and all five targets present (Figure S8d).

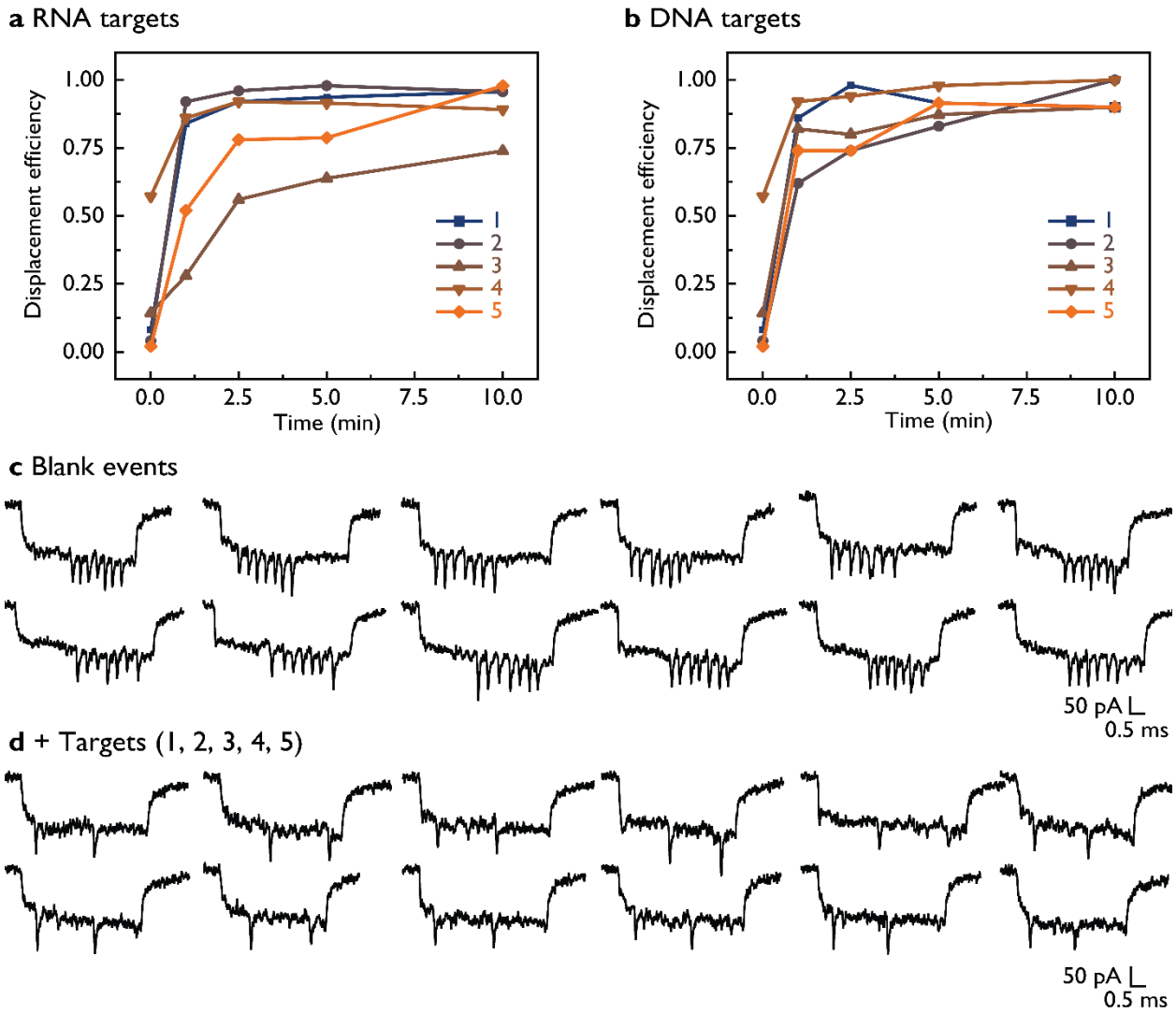

Figure S8. Kinetics of the toehold strand-displacement reaction (SDR) using RNA and DNA targets. Displacement efficiency for five different RNA and DNA targets are plotted in a) and b), respectively. c) Blank (no targets added) nanopore events indicate correct nanobait assembly. d) After the SDR with five targets added all five target-specific downward signals diminish.

We have measured single-molecule kinetics of strand displacement reaction over 9 h for RNA targets (Figure S9). This experiment is performed with the diluted nanobait sample and in 1:1 ratio nanobait to target and with typical 10 min incubation for the SDR. We have obtained from 1150 to 2860 events per hour slot (~18000 events) and the first fifty events were analyzed after each hour and the average value is plotted in Figure S9.

We can observe a general trend of increasing displacement efficiency for all five targets (Figure S9).

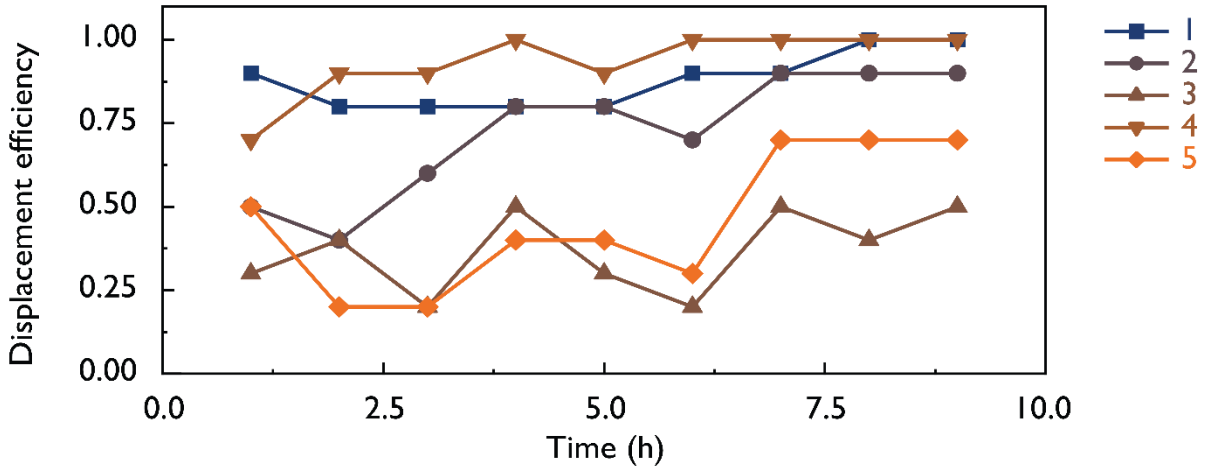

Figure S9. Single-molecule kinetics of the toehold strand-displacement reaction (SDR) using RNA targets.

Supplementary Table S13. Presence of peaks at their respective sites for the multiple SARS-CoV-2 target identification.

Target/Case	Control (no targets)	Standard error	Target present	Standard error
H1	0.08	0.14	0.92	0.08
H2	0.10	0.16	0.90	0.22
H3	0.13	0.18	0.87	0.14
H4	0.38	0.11	0.62	0.08
H5	0.08	0.14	0.92	0.12

Supplementary Table S14. Target sequences for the multiple SARS-CoV-2 target identification.

Strand name	Sequence (5’ → 3’)	Length (nt)
H1	TGATTGTGAAGAAGAAGAGT	20
H2	AAGAAAGGAGCTAAATTGTT	20
H3	AGAGTTGATTTTTGTGGAAA	20
H4	TGGTGTTTATTCTGTTATTT	20
H5	GGTAAAGTTGAGGGTTGTAT	20

Supplementary Table S15. 3’ Biotinylated strand sequences for SARS-CoV-2 target identification in a patient sample.

Strand name	Sequence (5’ → 3’)	Length (nt)
bH1	TGAAGAAGAAGAGT /3’-biotin/	14
bH2	GGAGCTAAATTGTT /3’-biotin/	14
bH3	GATTTTTGTGGAAA /3’-biotin/	14
bH4	TTATTCTGTTATTT /3’-biotin/	14
bH5	GTTGAGGGTTGTAT /3’-biotin/	14

Supplementary Table S16. Capture strand sequences for the multiple SARS-CoV-2 target identification.

Strand name	Sequence (5’ → 3’)	Length (nt)
cH1_42	TTCGACAACTCGTATTAAATCCTTTGCCCGAACGTTAT TTTTT ACTCTTCTTCTTCACAATCA	63
cH2_55	GTGAGTGAATAACCTTGCTTCTGTAAATCGTCGCTATT TTTTT AACAATTTAGCTCCTTTCTT	63

cH3_68	AGAATATAAAGTACCGACAAAAGGTAAAGTAATTCTGT TTTTT TTTCCACAAAAATCAACTCT	63
cH4_81	TCCCAATCCAAATAAGAAACGATTTTTTGTTTAACGTC TTTTT AAATAACAGAATAAACACCA	63
cH5_94	CATTCAACCGATTGAGGGAGGGAAGGTAAATATTGACG TTTTT ATACAACCCTCAACTTTACC	63

Section S9. Gel analysis of MS2 RNA cutting

Oligonucleotides A and B (Figure 4c) correspond to guide oligos TXA and TXB (X is the target name). Oligo C corresponds to cTX (X is the target name).

We treated MS2 RNA with a single target or with all three targets together to visualize site-specific cutting of RNA. We analyzed these samples using agarose gel electrophoresis (Figure S10). After MS2 RNA cutting for all three sites, we can observe expected lane mobility.

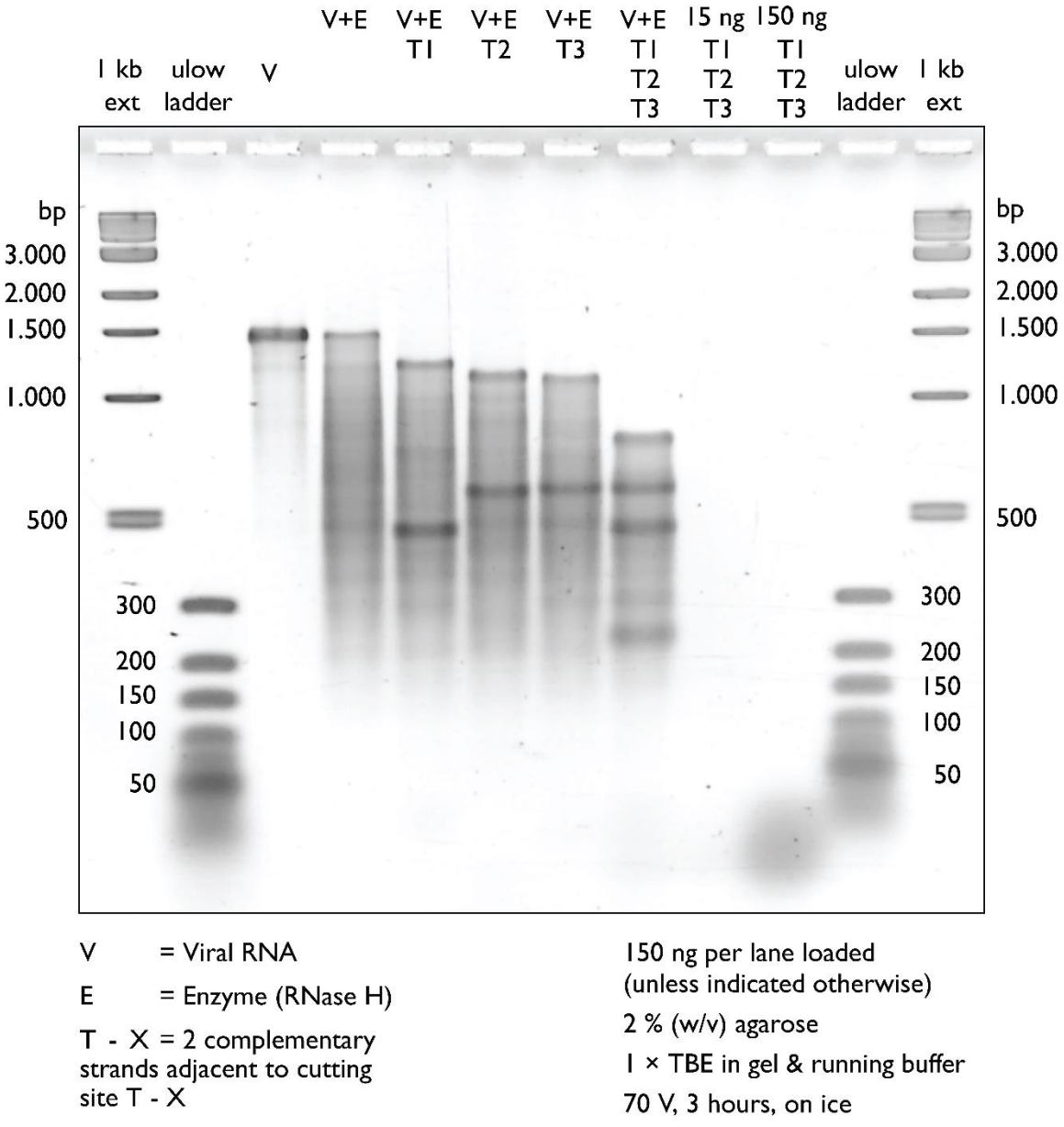

Figure S10. Agarose gel analysis of RNase H cutting of MS2 viral RNA.

We tested the mobility of targets, guide oligos, and capture oligos with non-denaturing polyacrylamide gel electrophoresis (PAGE) analysis (Figure S11). Even though targets and guide oligos have the same length they have different band mobility. This result indicates that mobility can be related to the sequence. We employed this advantage to detect each target in the background of guide oligos.

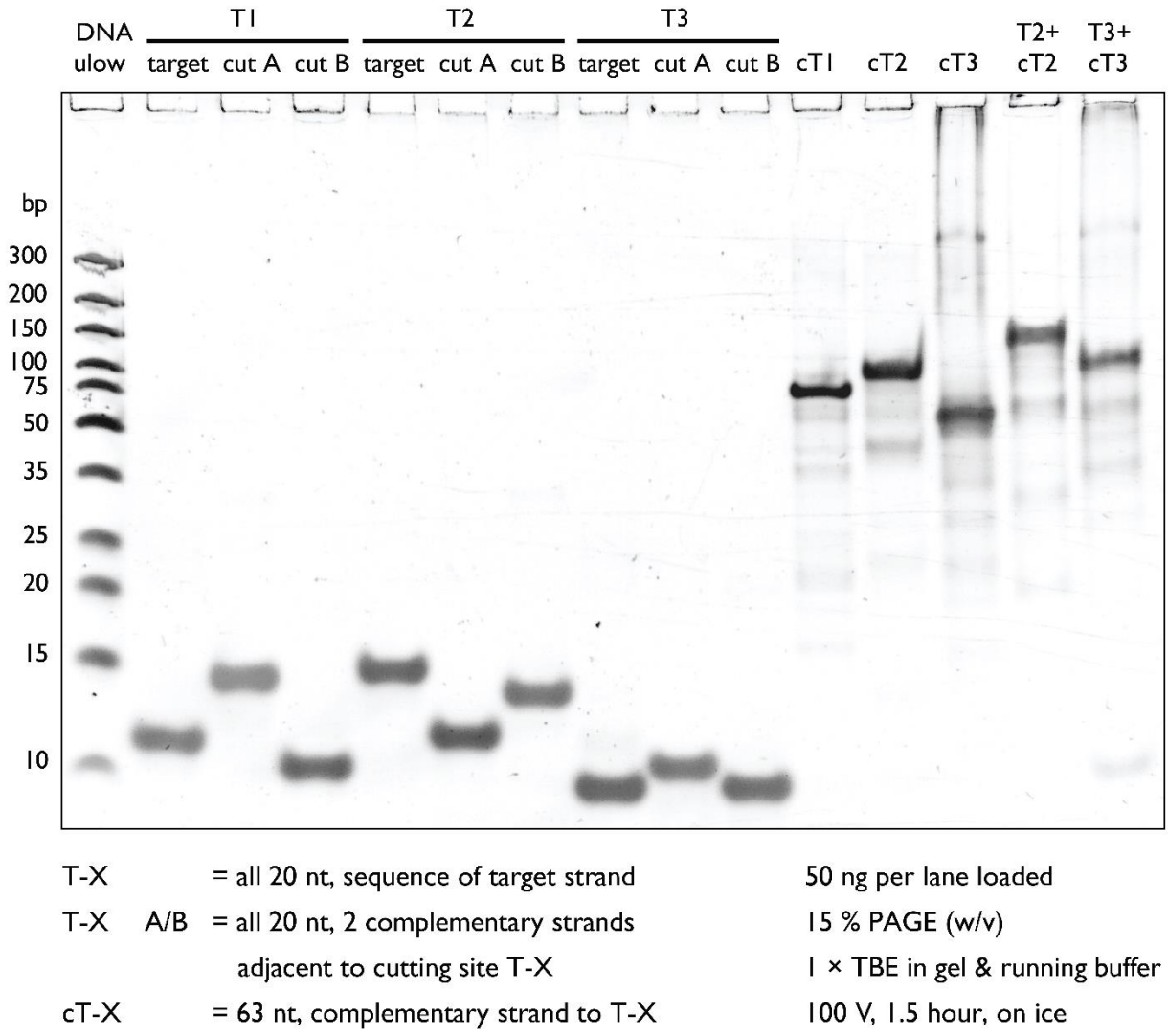

Figure S11. PAGE gel analysis of oligonucleotides used for MS2 RNase H cutting, target strands, and complementary capture strands.

We performed a control PAGE analysis by treating MS2 RNA with RNase H cutting without guide oligos. Here, we tested if targets have significant binding to enzyme-treated RNA (Figure S12).

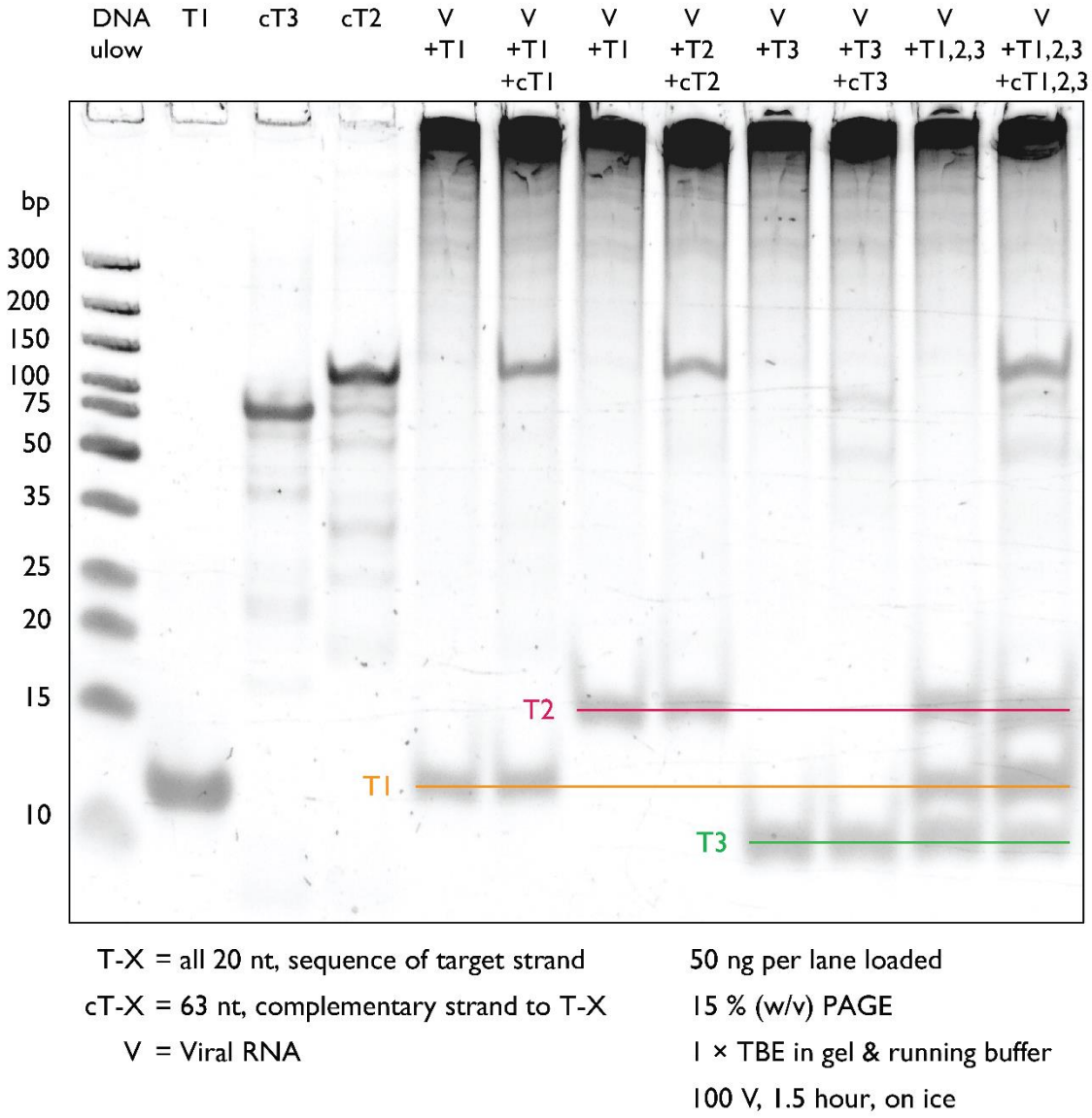

Figure S12. PAGE gel analysis of oligonucleotide mobility in a background of MS2 RNA treated with RNase H without added guide oligos.

Previously, we have shown that MS2 RNA is cut in fragments of the desired size with 100 % efficiency. However, the release of target RNAs from cut MS2 RNA cannot be tested using this gel. In Figure S13 we tested if RNA target is free in solution (Figure S13). Once MS2 RNA is cut with one guide oligo, the target is absent (x T1A) and the T1A oligo is the only one visible. If both guide oligos are added for target T1 an additional band is visible on the gel. We wanted to validate that this band is the T1 target. This is performed by mixing cut MS2 with a complementary strand (cT1+30 T; the sequence is listed in Table S18) and observing a shift from the cT1+30 T strand.

In the case of the T2 target, we have not observed any additional band indicating that target M2 is probably bound to its position in MS2 RNA structure, as discussed in the main text.

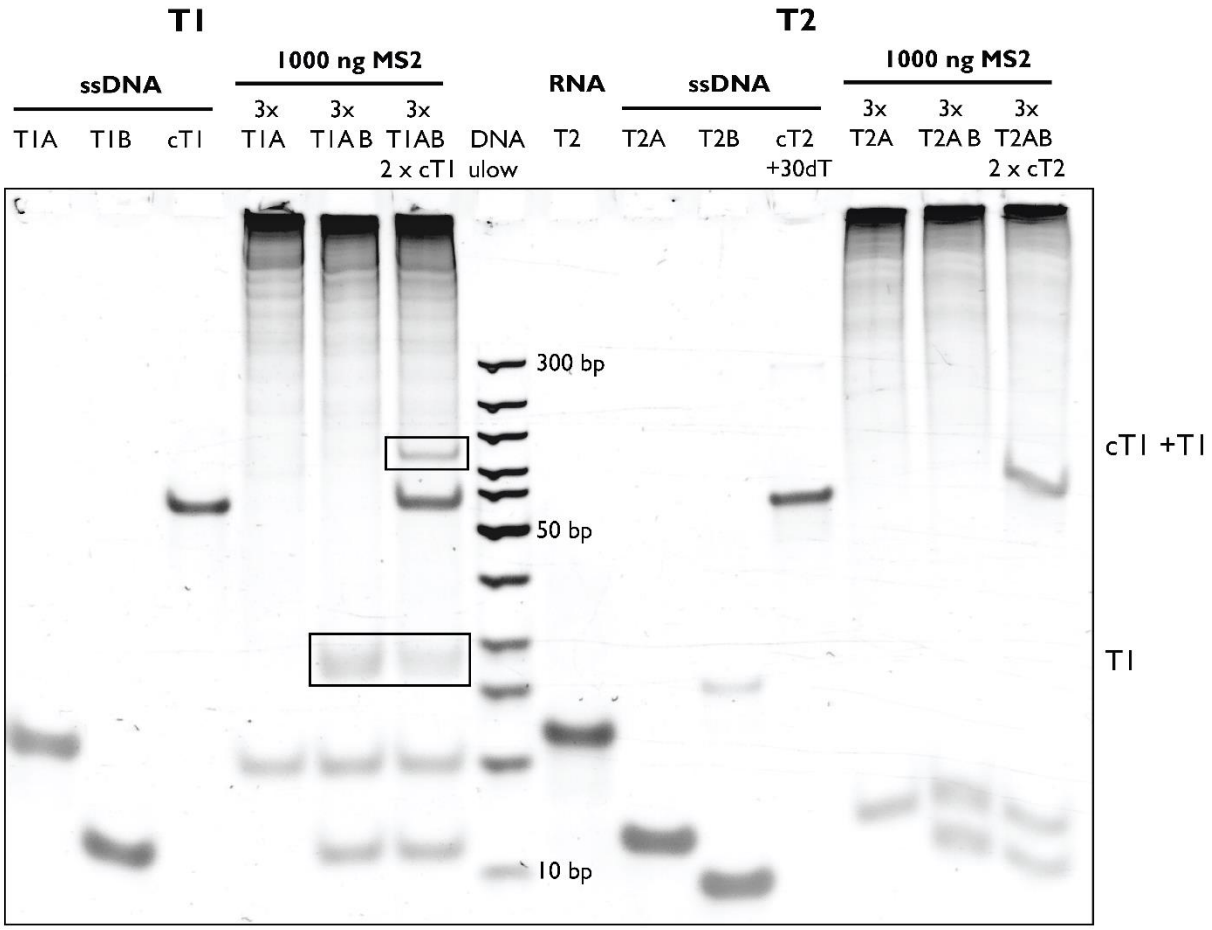

T-X = all 20 nt, sequence of target strand

T-X A/B = all 20 nt, 2 complementary strands adjacent to cutting site T-X

cT-X(+30 dT) = 63 nt, complementary strand to T-X

RNA M2	50 ng
T-X A & B	50 ng
cT-X	30 ng
MS2	1000 ng

15 % (w/v) PAGE

1 × TBE in gel & running buffer

100 V, 1.5 hour, on ice

Figure S13. PAGE gel analysis of target detection after MS2 RNA treated with RNase H with respective guide oligos for targets T1 and T2. DNA ulow lane corresponds to GeneRuler ultra low range DNA ladder (Thermo Fisher Scientific) with the lowest band has 10 bp and the highest band 300 bp.

Section S10. DNA nanobait for MS2 RNA target detection

Nanobait for MS2 virus is prepared as previously described in Section S2. Below, are listed sequences of capture sites (Table S16), biotin strand (Table S15), and target sequence (Table S14). In Table S17 are listed guide oligos for all targets.

We also show here additional nanopore events of nanobait without cut MS2 added (Figure S14a), and with cut MS2 RNA (Figure S14b). The nanobait and peaks resemble those presented in Figure 4b of the manuscript. These single-molecule events are obtained from three nanopore measurements.

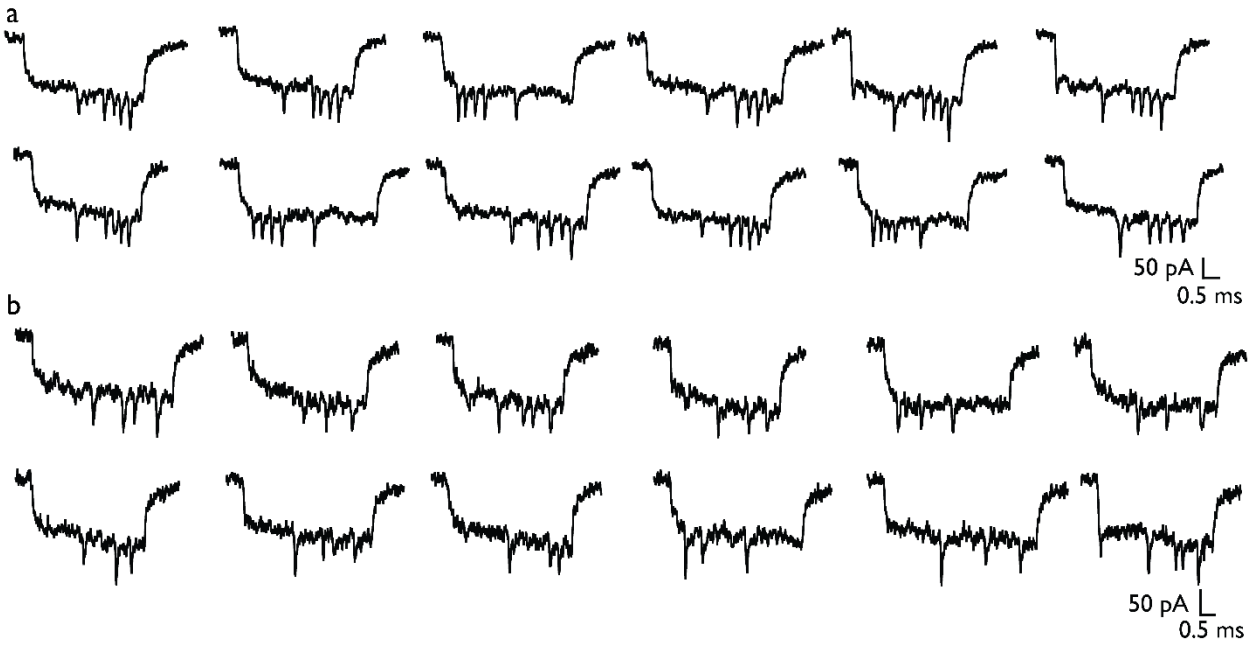

Figure S14. Example events for nanobait with cut MS2 RNA. a) Single-molecule nanobait events indicate that a) all three peaks are present, hence targets are not present, or b) peaks are absent, hence targets are present.

Supplementary Table S17. Presence of peaks at their respective sites for the multiple MS2 viral target identification.

Target/Case	Control (no targets)	Standard error	Target present	Standard error
T1	0.08	0.01	0.41	0.01

T2	0.11	0.04	0.25	0.04
T3	0.06	0.03	0.14	0.02

Supplementary Table S18. Target sequences for MS2 target identification.

Strand name	Sequence (5' → 3')
T1	ACCACTAATGAGTGATATCC
T2	TACCTGTAGGTAACATGCTC
T3	TCTGCATCCGATTCCATCTC

Supplementary Table S19. 3' Biotinylated strand sequences for MS2 target identification.

Strand name	Sequence (5' → 3')	Length (nt)
bT1	AATGAGTGATATCC/3'-biotin/	14
bT2	TAGGTAACATGCTC/3'-biotin/	14
bT3	TCCGATTCCATCTC/3'-biotin/	14

Supplementary Table S20. Capture strand sequences for MS2 target identification.

Strand name	Sequence (5' → 3')
cT1_42	TTCGACAACTCGTATTAAATCCTTTGCCCGAACGTTATTTTTT GGATATCACTCATTAGTGGT
cT2_55	GTGAGTGAATAACCTTGCTTCTGTAAATCGTCGCTATT TTTTT GAGCATGTTACCTACAGGTA
cT3_68	AGAATATAAAGTACCGACAAAAGGTAAAGTAATTCTGT TTTTT GAGATGGAATCGGATGCAGA

Supplementary Table S21. Guide oligo sequences for MS2 target identification.

Strand name	Sequence (5’ → 3’)
T1a	AACCAACCGAACTGCAACTC
T1b	AAGCATCTCATATGCACCCT
T2a	GGAGCCAGTCGACAACGAAT
T2b	ACGGGGGCCGTAAGGCCCTC
T3a	CGATAAGTCTATCGTCGCAA
T3b	AACTCCACACCAGGCGATCG

Supplementary Table S22. Complementary strands to MS2 targets with the 30 T-tail used for PAGE gel analysis.

Strand name	Sequence (5’ → 3’)
cM1_30T	TTTTTTTTTTTTTTTTTTTTTTTTTTTTTTGGATATCACTCATTAGTGGT
cM2_30T	TTTTTTTTTTTTTTTTTTTTTTTTTTTTTTGAGCATGTTACCTACAGGTA

Section S11. Detection of SARS-CoV-2 RNA targets from patient samples using DNA nanobait

Nanobait for SARS-CoV-2 virus is prepared as previously described in Section S2. Below, there are listed sequences of capture sites (Table S21), biotin strand (Table S20), and target sequence (Table S19). In Table S22 are listed guide oligos for all targets.

Supplementary Table S23. Target sequences for SARS-CoV-2 target identification in a patient sample.

Strand name	Sequence (5' → 3')
S1	CATCCTTACTGCGCTTCGAT
S2	CATTGCAACTGAGGGAGCCT
S3	AGACTCAGACTAATTCTCCT

Supplementary Table S24. 3' Biotinylated strand sequences for SARS-CoV-2 target identification in a patient sample.

Strand name	Sequence (5' → 3')	Length (nt)
bS1	TACTGCGCTTCGAT/3'-biotin/	14
bS2	AACTGAGGGAGCCT/3'-biotin/	14
bS3	AGACTAATTCTCCT/3'-biotin/	14

Supplementary Table S25. Capture strand sequences for SARS-CoV-2 target identification in a patient sample.

Strand name	Sequence (5' → 3')
cS1_43	TTCGACAACTCGTATTAAATCCTTTGCCCGAACGTTAT TTTTT ATCGAAGCGCAGTAAGGATG

cS2_55	GTGAGTGAATAACCTTGCTTCTGTAAATCGTCGCTATT TTTTT AGGCTCCCTCAGTTGCAATG
cS3_68	AGAATATAAAGTACCGACAAAAGGTAAAGTAATTCTGT TTTTT AGGAGAATTAGTCTGAGTCT

Supplementary Table S26. Guide DNA oligo sequences for SARS-CoV-2 target identification in patient samples.

Strand name	**Sequence (5' → 3')**
S1a	GCTAGTGTAACTAGCAAGAA
S1b	ATTGCAGCAGTACGCACACA
S2a	CGTTCTCCATTCTGGTTACT
S2b	GTGATCTTTTGGTGTATTCA
S3a	GATAACTAGCGCATATACCT
S3b	GCTACACTACGTGCCCGCCG

Section S12. Detection of SARS-CoV-2 RNA targets from patient samples using DNA nanobait and DNA flower as a label

The nanobait synthesis follows previously explained protocol. As shown in Figure S15, to construct the reference structures on the nanobait, staples 26-32 and 96-102 were substituted by the relevant dumbbell sequences (Table S24). To link the DNA flowers onto the nanobait, staple 43 was substituted by strand P43 and C43 (C43 was added during preparation of 7WJa, so only P43 was added here), staple 57 was substituted by strand C57 and P57, and staple 68 was substituted by strand cS3-68. The staples were accurately mixed as designed, and then the linear M13 scaffold was added into the solution (20 nM M13 scaffold, 60 nM staples, 120 nM dumbbell strands, and 120 nM P43, C57, P57, cS3-68). The mixture was heated to 70°C followed by a linear cooling ramp to 25°C over 50 minutes. 1 μL of 4 μM 7WJa, 7WJb, and 7WJc (DNA flowers) were added into the 40 μL nanobait solution and incubated at room temperature for 2 h. Finally, the resulted solution was diluted with a washing buffer (10 mM Tris-HCl, 0.5 $MgCl_2$, pH 8.0) to 500 μL and centrifuged at 6000 g for 10 min with an Amicon Ultra 100 kDa filter to remove the excess DNA strands and DNA flowers (repeated 3 times). About 35 μL of nanobait solution was obtained and quantified with a NanoDrop 2000 spectrophotometer.

The flower nanobait for the COVID-19 patient sample was diluted by TM buffer to 250 pM. 3.8 μL of a patient sample (positive or negative) was mixed with 0.2 μL of 250 pM nanobait, 0.5 μL of 100 mM $MgCl_2$, and 0.5 μL of 1M NaCl. The mixture (5 μL) was incubated at room temperature for 10 min and then diluted by 5 μL of 8 M LiCl and 20 μL of 4 M LiCl (in 1 × TE, pH 9.0) before nanopore measurement.

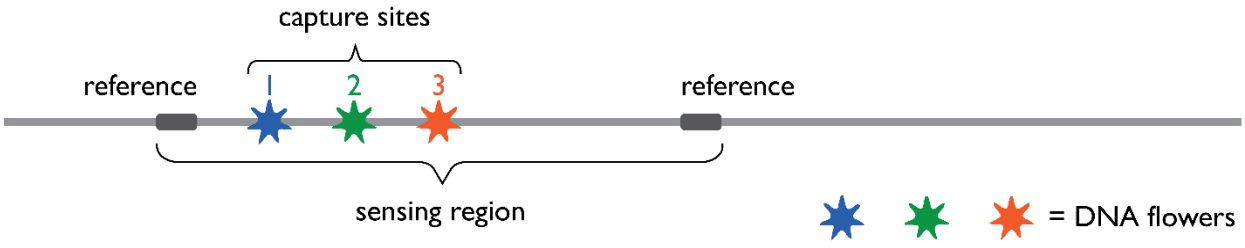

Figure S15. Design of nanobait with the DNA flower labels for testing COVID-19 patient sample. Each of references is represented by eleven DNA dumbbells.

Oligonucleotide sequences for DNA flower-based detection with nanobait are listed in Table S23. Example events for negative and positive SARS-CoV-2 patient samples obtained using DNA flowers are shown in Figure S16a and Figure S16b, respectively.

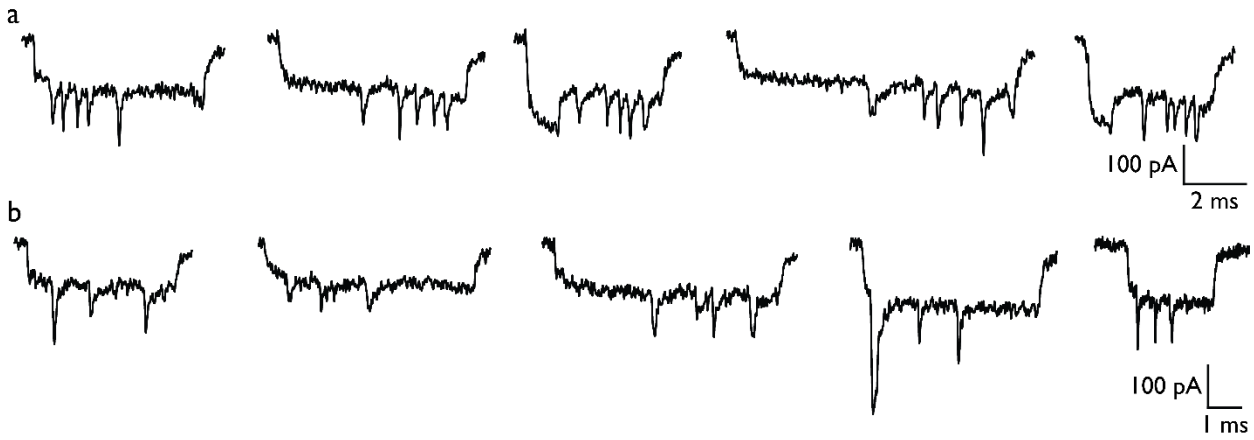

Figure S16. Example events of nanobait with DNA flower labels incubated with negative and positive SARS-CoV-2 patient samples (a and b, respectively).

Supplementary Table S27. Capture strand sequences for SARS-CoV-2 target identification in a patient sample using DNA flower as a label.

Strand name	Replaced oligo #	Sequence (5' → 3')
cFS1_43	43	TAATTTTAAAAGTTTGAGTA TT ATCGAAGCGCAGTA AGGATG
43+	43	ACATTATCATTTTGCGGA
cFS2_57	57	AGCTTAGATTAAGACGCTGA TT AGGCTCCCTCAGTT GCAATG
57+	57	GAAGAGTCAATAGTGAAT
cFS3_68	68	AGAATATAAAGTACCGACAAAAGGTAAAGTAATTCTGT TTTTT AGGAGAATTAGTCT GAGTCT

Supplementary Table S28. List of oligonucleotides that were replaced from Table S2. to assemble reference structures for nanobait with DNA flower. DNA dumbbell forming sequence is indicated in red.

Strand name	Sequence (5' → 3')	Length (nt)	Replaced oligo #
*REF 1.1	CTGAAAGCGTAAGAATACGTGGCACAGACAATATTTTTGAATGGCT	46	
*REF 1.2	ACATCACTTGTCCTCTTTTGAGGAACAAGTTTTCTTGTCCTGAGTAGA	48	
*REF 1.3	AGAACTCAAATCCTCTTTTGAGGAACAAGTTTTCTTGTCTATCGGCCT	48	
*REF 1.4	TGCTGGTAATTCCTCTTTTGAGGAACAAGTTTTCTTGTATCCAGAACA	48	
*REF 1.5	ATATTACCGCTCCTCTTTTGAGGAACAAGTTTTCTTGTCAGCCATTGC	48	
*REF 1.6	AACAGGAAAATCCTCTTTTGAGGAACAAGTTTTCTTGTACGCTCATGG	48	26-32
*REF 1.7	AAATACCTACTCCTCTTTTGAGGAACAAGTTTTCTTGTATTTTGACGC	48	
*REF 1.8	TCAATCGTCTTCCTCTTTTGAGGAACAAGTTTTCTTGTGAAATGGATT	48	
*REF 1.9	ATTTACATTGTCCTCTTTTGAGGAACAAGTTTTCTTGTGCAGATTCAC	48	
*REF 1.10	CAGTCACACGTCCTCTTTTGAGGAACAAGTTTTCTTGTACCAGTAATA	48	
*REF 1.11	AAAGGGACATTCCTCTTTTGAGGAACAAGTTTTCTTGTTCTGGCCAAC	48	
*REF 1.12	AGAGATAGAATCCTCTTTTGAGGAACAAGTTTTCTTGTCCCTTCTGAC	48	
*REF 2.1	CTTGAGCCATTCCTCTTTTGAGGAACAAGTTTTCTTGTTTGGGAATTA	48	
*REF 2.2	GAGCCAGCAATCCTCTTTTGAGGAACAAGTTTTCTTGTAATCACCAGT	20	
*REF 2.3	AGCACCATTATCCTCTTTTGAGGAACAAGTTTTCTTGTCCATTAGCAA	48	96-102
*REF 2.4	GGCCGGAAACTCCTCTTTTGAGGAACAAGTTTTCTTGTGTCACCAATG	48	
*REF 2.5	AAACCATCGATCCTCTTTTGAGGAACAAGTTTTCTTGTTAGCAGCACC	48	
*REF 2.6	GTAATCAGTATCCTCTTTTGAGGAACAAGTTTTCTTGTGCGACAGAAT	48	

*REF 2.7	CAAGTTTGCCTCCTCTTTTGAGGAACAAGTTTTCTTGTTTTAGCGTCA	48
*REF 2.8	GACTGTAGCGTCCTCTTTTGAGGAACAAGTTTTCTTGTCGTTTTCATC	48
*REF 2.9	GGCATTTTCGTCCTCTTTTGAGGAACAAGTTTTCTTGTGTCATAGCCC	48
*REF 2.10	CCTTATTAGCTCCTCTTTTGAGGAACAAGTTTTCTTGTGTTTGCCATC	48
*REF 2.11	TTTTCATAATTCCTCTTTTGAGGAACAAGTTTTCTTGTCAAAATCACC	48
*REF 2.12	GGAACCAGAGCCACCACCGGAACCGCCTCCCTCAGAGCCGCCACCC	46

Section S13. Nanopore data analysis

Data analysis of nanopore current traces is performed as previously described [3,6,16]. The data analysis workflow is shown in Figure S17. Firstly, in a raw ionic current trace, our home-built LabView script identifies events by specifying the event duration range and the current threshold. In the next step, nanobait events are separated from isolated events with too small and too large event charge deficit (ECD). Nanobaits can translocate through the nanopore as unfolded or folded (Figure S17). Here, we identify nanobait sensing region and calculate displacement efficiency for each site.

Nanopore events can be analyzed with the convolutional neural network QuipuNet following the procedure outlined in Figure S17. Its event detection is much faster with the rate of 1600 events/s, making it appropriate for instantaneous, real-time data analysis[16] that is not achievable with the other detection methods[17–19].

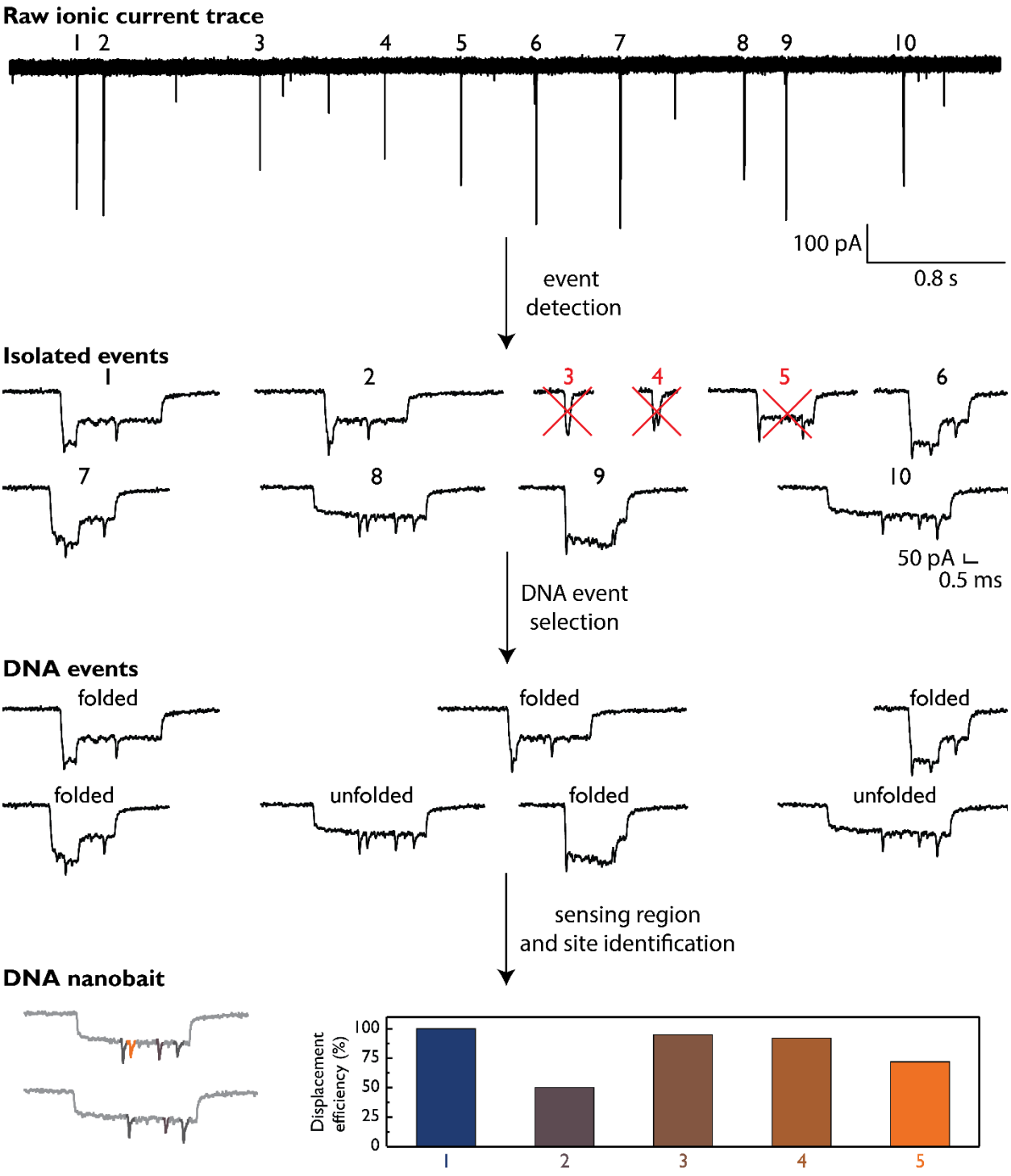

Figure S17. Nanopore data analysis workflow. The data analysis starts by searching for single-molecule events from the raw nanopore ionic current traces. Event's duration, current drop, and event charge deficit (ECD i.e. event's surface area) are parameters that further separate events from DNA events. DNA events in nanopore measurements can include bent or folded events and

linear or unfolded events. The next analysis step includes identifying the sensing region (marked by two references) and the absence of the peaks at their respective sites. In the last step, we calculate the mean and errors from multiple single-molecule events (from multiple nanopores), that are subtracted to the control measurement and presented as the displacement efficiency in the bar chart.

Section S14. Nanopore statistics

All nanopore measurements are listed in Table S25 with characteristics of both nanopores used and sample. In all measurements, the first fifty unfolded nanobaits were used for the displacement efficiency calculations unless otherwise specified. All measurements were obtained under an applied field of 600 mV and the respective ionic current value is indicated in Table S25. Only nanopores with the linear current-voltage curve and the noise root mean square (RMS) of < 7 pA were used for nanopore measurements.

Supplementary Table S29. Nanopore measurement details for all experiments presented in this study.

Nanopore measurement	DNA nanobait type / sample name	Current at 600 mV (nA)	Target present	RNase H cutting	Human total RNA	Patient sample	Excess of targets (times)	Incubation time (min)
1	Blank	10	/	/	/	/	10	10
2	Blank	11	/	/	/	/	10	10
3	Blank	14.5	/	/	/	/	10	10
4	Blank	14	/	/	/	/	10	10
5	Blank	11	/	/	/	/	10	10
6	Blank	7	/	/	/	/	10	10
7	Blank	12	/	/	/	/	10	10
8	Blank	8	/	/	/	/	10	10
9	H1-H5	12.4	five targets	/	/	/	10	10
10	H1-H5	9.8	five targets	/	/	/	10	10
11	H1-H5	12.15	five targets	/	/	/	10	10
12	H1-H5	12.3	five targets	/	/	/	10	10
13	total RNA + Nanobait	9.5	/	/	yes	/	10	10
14	total RNA + Nanobait	10.2	/	/	yes	/	10	10
15	total RNA + Nanobait	10	/	/	yes	/	10	10
16	total RNA + Nanobait+targets	9.4	five targets	/	yes	/	10	10
17	total RNA + Nanobait+targets	9.25	five targets	/	yes	/	10	10
18	total RNA + Nanobait+targets	10.5	five targets	/	yes	/	10	10

19	Nanobait + negative covid sample a53	9	/	/	/	negative	NA	10
20	Nanobait + negative covid sample a53	9	/	/	/	negative	NA	10
21	Nanobait + negative covid sample a53	10.6	/	/	/	negative	NA	10
22	Nanobait + negative covid sample a55	10.2	/	/	/	negative	NA	10
23	Nanobait + negative covid sample a55	11	/	/	/	negative	NA	10
24	Nanobait + negative covid sample a55	8.72	/	/	/	negative	NA	10
25	Nanobait + negative covid sample+targets	10.5	all targets	/	/	negative	NA	10
26	Nanobait + negative covid sample+targets	10.25	all targets	/	/	negative	NA	10
27	Nanobait + negative covid sample+targets	11	all targets	/	/	negative	NA	10
28	Nanobait + negative covid sample+RNaseH cutting	10.2	/	yes	/	negative	NA	10
29	Nanobait + negative covid sample+RNaseH cutting	9.8	/	yes	/	negative	NA	10
30	kinetics 1 min DNA	9.8	all targets	/	/	/	10	1
31	kinetics 2.5 min DNA	10.9	all targets	/	/	/	10	2.5
32	kinetics 5 min DNA	11.2	all targets	/	/	/	10	5
33	kinetics 10 min DNA	10	all targets	/	/	/	10	10
34	kinetics 1 min RNA	12	all targets	/	/	/	10	1
35	kinetics 2.5 min RNA	12.4	all targets	/	/	/	10	2.5
36	kinetics 5 min RNA	12.2	all targets	/	/	/	10	5
37	kinetics 10 min RNA	10	all targets	/	/	/	10	10
38	Nanobait for MS2 blank	12	/	/	/	/	10	10
39	Nanobait for MS2 blank	11	/	/	/	/	10	10
40	Nanobait for MS2 blank	11	/	/	/	/	10	10
41	Nanobait for MS2 blank+targets	11.58	all targets	/	/	/	10	10
42	Nanobait for MS2 blank+targets	10.8	all targets	/	/	/	10	10

43	Nanobait for MS2 blank+RnaseH cutting	10	/	yes	/	/	10	10
44	Nanobait for MS2 blank+RnaseH cutting	12.5	/	yes	/	/	10	10
45	Nanobait for patient covid sample	11	/	/	/	/	10	10
46	Nanobait for patient covid sample	10.7	/	/	/	/	10	10
47	Nanobait for patient covid sample+EU reference	16.2	/	yes	/	positive EU reference	NA	10
48	Nanobait for patient covid sample+EU reference	7.2	/	yes	/	positive EU reference	NA	10
49	Nanobait for patient covid sample+negative sample	9.9	/	yes	/	negative	NA	10
50	Nanobait for patient covid sample+positive sample	9.8	/	yes	/	positive	NA	10
51	Nanobait for patient covid sample+positive sample	10.7	/	yes	/	positive	NA	10
52	Nanobait for patient covid sample+positive sample	10.4	/	yes	/	positive	NA	10
53	Nanobait for patient covid sample with DNA flower	6.98	/	/	/	/	10	10
54	Nanobait for patient covid sample with DNA flower+negative sample	11.4	/	yes	/	negative	NA	10
55	Nanobait for patient covid sample with DNA flower+negative sample	11.18	/	yes	/	negative	NA	10
56	Nanobait for patient covid sample with DNA flower	11.44	/	yes	/	positive	NA	10
57	Nanobait for patient covid sample with DNA flower	9.89	/	yes	/	positive	NA	10
58	Nanobait for patient covid sample with DNA flower	10.1	/	yes	/	positive	NA	10

59	Nanobait for multiple viruses blank	9	/	/	/	/	10	10
60	Nanobait for multiple viruses blank	7.5	/	/	/	/	10	10
61	Nanobait for multiple viruses blank	8.5	/	/	/	/	10	10
62	Nanobait for multiple viruses blank+all targets	8.8	all targets	/	/	/	10	10
63	Nanobait for multiple viruses blank+all targets	8	all targets	/	/	/	10	10
64	Nanobait for multiple viruses blank+SARS-CoV-2 target	8.6	SARS-CoV-2	/	/	/	10	10
65	Nanobait for multiple viruses blank+SARS-CoV-2 target	10.15	SARS-CoV-2	/	/	/	10	10
66	Nanobait for multiple viruses blank+SARS-CoV-2 target	11	SARS-CoV-2	/	/	/	10	10
67	Nanobait for multiple viruses blank+Influenza target	8.99	Influenza	/	/	/	10	10
68	Nanobait for multiple viruses blank+Influenza target	9.42	Influenza	/	/	/	10	10
69	Nanobait for multiple viruses blank+Influenza target	14.8	Influenza	/	/	/	10	10
70	Nanobait for multiple viruses blank+RSV target	9.54	RSV	/	/	/	10	10
71	Nanobait for multiple viruses blank+RSV target	15.15	RSV	/	/	/	10	10
72	Nanobait for multiple viruses blank+RSV target	9.34	RSV	/	/	/	10	10
73	Nanobait for multiple viruses blank+Parainfluenza target	9.6	Parainfluenza	/	/	/	10	10
74	Nanobait for multiple viruses	9.67	Parainfluenza	/	/	/	10	10

	blank+Parainfluenza target							
75	Nanobait for multiple viruses blank+Parainfluenza target	15.2	Parainfluenza	/	/	/	10	10
76	Nanobait for multiple viruses blank+Rhinoviruses target	8.9	Rhinoviruses	/	/	/	10	10
77	Nanobait for multiple viruses blank+Rhinoviruses target	15.5	Rhinoviruses	/	/	/	10	10
78	Nanobait for multiple viruses blank+Rhinoviruses target	9.74	Rhinoviruses	/	/	/	10	10
79	Nanobait for variants blank	9.01	/	/	/	/	10	10
80	Nanobait for variants blank	9.7	/	/	/	/	10	10
81	Nanobait for variants blank	8.52	/	/	/	/	10	10
82	Nanobait for variants blank + WT targets	8.5	all targets	/	/	/	10	10
83	Nanobait for variants blank + WT targets	8.5	all targets	/	/	/	10	10
84	Nanobait for variants blank + WT targets	7.8	all targets	/	/	/	10	10
85	Nanobait for variants blank + variant targets	8.8	all targets	/	/	/	10	10
86	Nanobait for variants blank + variant targets	9.03	all targets	/	/	/	10	10
87	Nanobait for variants blank + variant targets	9	all targets	/	/	/	10	10
88	Nanobait for variants+Wuhan variant target	11.5	Wuhan	/	/	/	10	10
89	Nanobait for variants+Wuhan variant target	10.5	Wuhan	/	/	/	10	10
90	Nanobait for variants+Indian variant target	10	Indian	/	/	/	10	10
91	Nanobait for variants+Indian variant target	10	Indian	/	/	/	10	10

92	Nanobait for variants+European variant target	10.1	European	/	/	/	10	10
93	Nanobait for variants+European variant target	13.75	European	/	/	/	10	10
94	Nanobait for variants+British variant target	10.68	British	/	/	/	10	10
95	Nanobait for variants+British variant target	8.3	British	/	/	/	10	10
96	Nanobait for variants+South African variant target	9.5	South African	/	/	/	10	10
97	Nanobait for variants+South African variant target	9.7	South African	/	/	/	10	10

REFERENCES

1. Fairhead, M., Krndija, D., Lowe, E. D. & Howarth, M. Plug-and-play pairing via defined divalent streptavidins. *Journal of Molecular Biology* **426**, 199–214 (2014).

2. Zhu, J., Ermann, N., Chen, K. & Keyser, U. F. Image encoding using multi-level DNA barcodes with nanopore readout. *Small* **17**, 2100711 (2021).

3. Bell, N. A. W. & Keyser, U. F. Digitally encoded DNA nanostructures for multiplexed, single-molecule protein sensing with nanopores. *Nature Nanotechnology* **11**, 645–651 (2016).

4. Stahl, E., Martin, T. G., Praetorius, F. & Dietz, H. Facile and scalable preparation of pure and dense DNA origami solutions. *Angewandte Chemie International Edition* **53**, 12735–12740 (2014).

5. Ohmann, A. *et al.* Controlling aggregation of cholesterol-modified DNA nanostructures. *Nucleic acids research* **47**, 11441–11451 (2019).

6. Bošković, F., Ohmann, A., Keyser, U. F. & Chen, K. DNA Structural barcode copying and random access. *Small Structures* **2**, 2000144 (2021).

7. Chen, K., Zhu, J., Bošković, F. & Keyser, U. F. Nanopore-based DNA hard drives for rewritable and secure data storage. *Nano Letters* **20**, 3754–3760 (2020).

8. Schindelin, J. *et al.* Fiji: An open-source platform for biological-image analysis. *Nature Methods* **9**, 676–682 (2012).

9. Lu, X. *et al.* Real-time reverse transcription-PCR assay for comprehensive detection of human rhinoviruses. *Journal of Clinical Microbiology* **46**, 533–539 (2008).

10. Templeton, K. E., Scheltinga, S. A., Beersma, M. F. C., Kroes, A. C. M. & Claas, E. C. J. Rapid and sensitive method using multiplex real-time PCR for diagnosis of infections by Influenza A and Influenza B viruses, Respiratory Syncytial Virus, and Parainfluenza Viruses 1, 2, 3, and 4. *Journal of Clinical Microbiology* **42**, 1564–1569 (2004).

11. Wu, F. *et al.* A new coronavirus associated with human respiratory disease in China. *Nature 2020 579:7798* **579**, 265–269 (2020).

12. https://www.who.int/influenza/gisrs_laboratory/WHO_information_for_the_molecular_detection_of_influenza_viruses_20171023_Final.pdf.

13. Shirato, K. *et al.* Diagnosis of human respiratory syncytial virus infection using reverse transcription loop-mediated isothermal amplification. *Journal of Virological Methods* **139**, 78–84 (2007).

14. Konings, F. *et al.* SARS-CoV-2 Variants of Interest and Concern naming scheme conducive for global discourse. *Nature Microbiology* **6**, 821–823 (2021).

15. Rambaut, A. *et al.* A dynamic nomenclature proposal for SARS-CoV-2 lineages to assist genomic epidemiology. *Nature Microbiology* **5**, 1403–1407 (2020).

16. Misiunas, K., Ermann, N. & Keyser, U. F. QuipuNet: Convolutional neural network for single-molecule nanopore sensing. *Nano Letters* **18**, 4040–4045 (2018).

17. ECDC & WHO. *Methods for the detection and identification of SARS-CoV-2 variants*. (2021).

18. Caliendo, A. M. Multiplex PCR and emerging technologies for the detection of respiratory pathogens. *Clinical Infectious Diseases* **52**, 326–330 (2011).

19. Zhou, L. *et al.* Programmable low-cost DNA-based platform for viral RNA detection. *Science Advances* **6**, eabc6246 (2020).